

Responses to the Comments of the Anonymous Referee #1

We very much appreciate the constructive comments and suggestions from this reviewer. Our point-by-point responses to the reviewer's comments are as follows (the reviewer's comments are marked in *Italic font*).

Comments:

This study investigates the impact of biomass burning aerosols on convective systems in the Sumatra and Borneo regions of Southeast Asia using the WRF-Chem model. Considering the large uncertainty in the interactions between aerosols, particularly those from biomass burning, and convective clouds, this study advances our understanding of the complicated and competing physical processes that governs the net effect of biomass-burning aerosols. The manuscript is generally well written. I think it can be considered for publication after the author addresses the following comments and suggestions.

1. Abstract: The descriptions after Line 45 are much too general. The author mentioned several times that fire aerosols have “significant/substantial impacts” on convection. What exactly are these impacts? I believe the author should summarize their main findings here so that the abstract can be more informative.

We thank the reviewer's suggestion. We have modified the abstract as: “Results from selected cases of convective events have shown significant impacts of fire aerosols specifically on the weak convections by increasing the quantities of hydrometeors and rainfall in both Sumatra and Borneo regions. Statistical analysis over the fire season also suggests that fire aerosols have impacts on the nocturnal convections associated with the local anticyclonic circulation in the western Borneo and then weakened the nocturnal rainfall intensity by about 9%. Such an effect is likely come from the near surface heating by absorbing aerosols emitted from fires that could weaken land breezes and thus the convergence of anticyclonic circulation.”

2. Line 173-175: How did you treat emissions from the flaming vs smoldering phases when calculating plume rise? A previous study (Shi et al., 2019, JGR-Atmospheres, DOI 10.1029/2019JD030472) has shown that the fraction of smoldering-phase emissions has a large impact on plume rise and fire-induced aerosol concentrations.

The current plume rise algorithm in WRF-Chem is based on the burning vegetation types not burning phases. In the reality, most peatland fires burn in smoldering-phase and most fire aerosols concentrate near surface. Shi et al. (2019) pointed out that not considering the characteristics of smoldering phase of burning in the model could lead to underestimated fire emissions and thus near surface fire aerosol concentration.

Our study has considered the first issue (the vegetation types) and we have made corresponding modification to WRF-Chem plume model. As mentioned in the manuscript, for peatland fire, we have set its heat flux as 4.4 kW m^{-2} , which is the same as that of savanna burning while differs significantly from that of the tropical forest burning in 30 kW m^{-2} . Furthermore, we have limited the plume injection height of peat fire by a ceiling of 700 m above

the ground based on remote sensing retrieval from Tosca et al. (2011). The injection height for tropical peat fire in our modeling was thus derived based on this new algorithm. We agree with the reviewer that the phase of burning should be considered more carefully in future efforts in deriving fire emission inventory. We have added a sentence in Lines 187-190 of the manuscript as: “Note that the current fire emission inventories could underestimate near surface fire aerosol concentration by ignoring some of the characteristics of smoldering burning as well (Shi et al., 2019).”

3. Line 185-186: I think it's not accurate to use “fossil fuel emissions” here. “Anthropogenic emissions” may be a better term. Many anthropogenic emissions do not originate from fossil fuels, such as VOC emissions from solvent use, NH₃ emissions from agricultural activities, and emissions from household biomass fuels.

We have modified the sentence to “Two numerical simulations, both included anthropogenic emissions (mainly fossil fuel emissions) while either with and without the biomass burning emissions (labeled as FFBB and FF, respectively) ...”

4. Line 191-193: This is an important point. You may want to show the data in SI.

We have added Fig. S1, the time series of domain-averaged monthly mean PM_{2.5} emissions from FINN and precipitation rate from TRMM dataset, in the supplement.

5. Section 3.1.2: Since fire emissions have a large day-to-day variability, I think the monthly mean AOD may not be suitable for evaluating the model performance. I suggest to use daily product (MOD08_D3) instead. Also, the author argues that the higher simulated AOD than observations is because “a high spatiotemporal resolution in our simulation enables the model to capture episodic fire events better”. I think comparing with daily AOD observations could help to confirm whether this argument is true or not.

We appreciate and actually agree on the reviewer’s point that fire emissions have a large day-to-day variability. However, due to the frequent appearance of convective systems, MODIS AOD data are often derived based on limited non-cloudy pixels in this region. In this sense, we believe that the comparison of MODIS AOD in a longer period (here we select for monthly) might better serve the purpose. In our pervious study, we have performed more quantitative comparisons of fire pollutants between modeled results and ground-based observations. In Lee et al. (2018), the comparisons of daily PM₁₀, CO, O₃ and visibility have demonstrated that the model is capable to capture episodic fire events during a long-term simulation.

6. Line 303: but smaller number?

The process of cloud droplet collection by rain increases the mass of rain while causes no change to the number of raindrops. We have modified the sentence to “Larger raindrops combining with smaller cloud droplets in FFBB can enhance the efficiency of cloud droplet collection by rain and thus increase rain water mass but cause no change to the number of raindrops, possibly compensating the decrease of rain water mass resulted from a lowered autoconversion.”

7. Line 307-308: Why do the mass concentration of snow and graupel increase significantly? Due to the aerosol invigoration effect? You need to explain.

We have added following sentences to explain the change of snow and graupel mass concentration in Lines 335-343 of the revised manuscript:
“Our result is consistent with that of Lin et al. (2006), which suggested that biomass burning aerosols could invigorate convection and then increase precipitation based on satellite observations. The aerosol invigoration effect is referred to such a hypothetical process that increasing number of smaller cloud droplets due to higher aerosol concentration would reduce the efficiency of raindrop formation from self-collection among cloud droplets, and thus further slowdown the loss of these small droplets from being collected by larger raindrops and allow more of them reach high altitudes, where they would eventually collected by ice particles through riming, causing release of latent heat to enhance updraft.”

8. Line 317-321, 351-353: Why do the aerosol impacts on stronger and weaker convective systems quite different? You should explain briefly here since the discussions in Sections 3.3 and 3.4 are far away. I think your finding that fire aerosols tend to invigorate weak convection but suppress deep convection is generally consistent with and could be better supported by previous observation-based studies (e.g., Jiang et al., 2018, Nature Communications, DOI 10.1038/s41467-018-06280-4; Zhao et al., 2018, GRL, DOI 10.1002/2018GL077261), which showed that smoke aerosols generally suppress deep convection and convection-generated ice clouds.

We thank the reviewer’s suggestion. We have added the following sentences in Lines 396-409 of the revised manuscript:
“Our results show that fire aerosols tend to invigorate weak convection but suppress deep convection in both Sumatra region (r1) and Borneo region (r2). As mentioned before, increasing the number of smaller cloud droplets due to higher aerosol concentration resulted from fire would reduce the efficiency of raindrop formation through the warm-rain processes, thus allowing more cloud droplets reach high altitudes to be eventually collected by ice particles through riming, causing release of latent heat to invigorate updraft while enhancing precipitation through melting of fallen ice particles (Wang, 2005). These processes appear to be more effective to weak convections than deep convections and were in fact well-simulated in the former cases. The results are also consistent with some previous observation-based studies (Jiang et al., 2018; Zhao et al., 2018). Jiang et al. (2018) and Zhao et al. (2018) both concluded that an increase of fire aerosols generally reduces cloud optical thickness of deep convection while Zhao et al. (2018) further showed that fire aerosols tend to invigorate weak convection for small-to-moderate aerosol loadings.”

9. Line 381-408: This part is difficult to follow and should be better organized. The author intends to investigate the dependency of the aerosol impact on convective strength (Line 381-382). This question is discussed for r1, but not clearly for r2. From the current text, I am not sure how the aerosol impacts differ for convective systems with different strength in r2. The same problem exists in the conclusion section. Also, why do you introduce daily maximum and

minimum rainfall? A few transitional sentences are needed. Line 391-392: Better to mention clearly that this refers to r1.

We have made an effort to clarify the commented discussions in Lines 431-448 of the revised manuscript:

“In Sect. 3.2, we have discussed the significant rainfall increase occurred in the weak convective systems after adding fire aerosols due to aerosol invigoration effect. On one hand, regardless the strength of convection, the mean 3-hourly rainfall during the fire periods is 1.06 ± 0.85 mm in FF and 1.09 ± 0.86 mm in FFBB over the Sumatra region (r1), and statistically it does not change significantly in responding to fire aerosols. The rainfall difference in the Borneo region (r2) between FF and FFBB is also insignificant (1.32 ± 1.20 mm 3hrs^{-1} in FF versus 1.35 ± 1.14 mm 3hrs^{-1} in FFBB). On the other hand, we have found that the impacts of fire aerosols appear in several other rainfall patterns. For instance, the daily maximum and minimum rainfalls display clear differences between the FFBB and FF simulations, specifically in r2 rather than in r1 (Fig. 9). While for r1, the impacts of fire aerosol are reflected in event-wise statistics, e.g., higher event-wise maximum and minimum rainfall intensity in FFBB than in FF, identified in 30 out of 54 convective events in total. These are mostly weak convective events in r1. Interestingly, somewhat opposite to the rainfall statistics in r1, the intensity of event-wise maximum and minimum rainfall in r2 is higher in FF than in FFBB. The daily rainfall peak of 3-hr rainfall in r1 is mostly less than 3 mm; in comparison, one-third of convective events in r2 have daily maximum 3-hr rainfall exceeding 3 mm (Fig. 9c), suggesting that the convective systems in r2 tend to develop stronger than in r1 and the fire aerosols significantly suppress the maximum rainfall intensity of strong convections in r1. ...”

10. Figures 5, 6: Some texts in the figures are too small to be visible.

Texts in the figures have been modified in the revised manuscript.

Reference:

- Jiang, J.H. *et al.*, Contrasting effects on deep convective clouds by different types of aerosols, *Nature Communications* **9**(2018), p. 3874.
- Lee, H.-H. *et al.*, Impacts of air pollutants from fire and non-fire emissions on the regional air quality in Southeast Asia, *Atmos. Chem. Phys.* **18**(2018), pp. 6141-6156.
- Lin, J.C., Matsui, T., Pielke Sr., R.A., Kummerow, C., Effects of biomass-burning-derived aerosols on precipitation and clouds in the Amazon Basin: a satellite-based empirical study, *Journal of Geophysical Research: Atmospheres* **111**(2006).
- Shi, H. *et al.*, Modeling Study of the Air Quality Impact of Record-Breaking Southern California Wildfires in December 2017, *Journal of Geophysical Research: Atmospheres* **124**(2019), pp. 6554-6570.
- Wang, C., A modeling study of the response of tropical deep convection to the increase of cloud condensation nuclei concentration: 1. Dynamics and microphysics, *Journal of Geophysical Research: Atmospheres* **110**(2005), p. D21211.
- Zhao, B. *et al.*, Type-Dependent Responses of Ice Cloud Properties to Aerosols From Satellite Retrievals, *Geophysical Research Letters* **45**(2018), pp. 3297-3306.

Responses to the Comments of the Anonymous Referee #2

We very much appreciate the constructive comments and suggestions from this reviewer. Our point-by-point responses to the reviewer's comments are as follows (the reviewer's comments are marked in *Italic font*).

Comments:

This paper examines the impacts of biomass burning aerosols on convective systems over the northern Sumatra and the western Borneo in the Maritime Continent based on based on long-term WRF-Chem simulations. While the paper is well written and interesting, there are some concerns that need to be addressed before the paper being publishable.

(1) The resolution of inner domain at 5 km is still too coarse for simulating convective clouds.

We agree with the reviewer that 5 km is still not an ideally fine resolution for simulating convective clouds, although commonly previous studies have shown that WRF model with a similar resolution can still reflect many critical characteristics of deep convection without using convection parameterization (e.g., Wagner et al., 2018). Specifically, because of the purpose of this study and the availability of computational resource, we have decided to use a 5 km resolution with cumulus scheme off. Based on our model evaluation, especially the comparison of sounding profiles, the model under the current configuration can capture the major characters of the convective systems very well.

In the revised manuscript, we have added following sentences in Section 2.1, Lines 162-170:

“Owing to the main purpose of this study to reveal fire aerosol-convection interaction through modeling a large quantity of convective systems continually over a relatively long period, and the computational resource available to us as well, we have adopted a 5 km horizontal resolution which excluding cumulus parameterization scheme. Previous studies have shown that WRF model with a similar resolution without convection parameterization can still capture many critical characteristics of deep convection (Wagner et al., 2018). Our model evaluation, especially through the comparison of modeled results with sounding profiles, has demonstrated the same.”

(2) The section of selected cases analysis looks vague and needs more detailed analysis. The impacts of aerosol on precipitation are very complicated (different mechanisms on different clouds under different conditions). It is too bold to get the conclusion just based on three cases even with cloud types unknown. There are so many convective cases that could be categorized them and analyzed in detail.

We have made our best effort to clarify the related discussions in the revised manuscript (see also our response to the Reviewer #1). First of all, we have made it clear that our simulations and analyses cover all the different cases, though we have chosen to identify different aspects of the impacts of fire aerosols through a different sets of analyses, ranging from deriving case-wise statistics to performing seasonal analysis.

The analyses based on selected three cases from each of the two study regions are just one of these. To avoid the impression that our conclusions were drawn from only three cases, we have made several revisions in the manuscript. One of the revised discussions in Lines 429-448 are: “In Sect. 3.2, we have discussed the significant rainfall increase occurred in the weak convective systems after adding fire aerosols due to aerosol invigoration effect. On one hand, regardless the strength of convection, the mean 3-hourly rainfall during the fire periods is 1.06 ± 0.85 mm in FF and 1.09 ± 0.86 mm in FFBB over the Sumatra region (r1), and statistically it does not change significantly in responding to fire aerosols. The rainfall difference in the Borneo region (r2) between FF and FFBB is also insignificant (1.32 ± 1.20 mm 3hrs^{-1} in FF versus 1.35 ± 1.14 mm 3hrs^{-1} in FFBB). On the other hand, we have found that the impacts of fire aerosols appear in several other rainfall patterns. For instance, the daily maximum and minimum rainfalls display clear differences between the FFBB and FF simulations, specifically in r2 rather than in r1 (Fig. 9). While for r1, the impacts of fire aerosol are reflected in event-wise statistics, e.g., higher event-wise maximum and minimum rainfall intensity in FFBB than in FF, identified in 30 out of 54 convective events in total. These are mostly weak convective events in r1. Interestingly, somewhat opposite to the rainfall statistics in r1, the intensity of event-wise maximum and minimum rainfall in r2 is higher in FF than in FFBB. The daily rainfall peak of 3-hr rainfall in r1 is mostly less than 3 mm; in comparison, one-third of convective events in r2 have daily maximum 3-hr rainfall exceeding 3 mm (Fig. 9c), suggesting that the convective systems in r2 tend to develop stronger than in r1 and the fire aerosols significantly suppress the maximum rainfall intensity of strong convections in r1. ...”

We have specifically enhanced our discussion regarding mechanisms of fire aerosol-convection impacts. An example is the following added discussion in Line 333-341: “Our result is consistent with that of Lin et al. (2006), which suggested that biomass burning aerosols could invigorate convection and then increase precipitation based on satellite observations. The aerosol invigoration effect is referred to such a hypothetical process that increasing number of smaller cloud droplets due to higher aerosol concentration would reduce the efficiency of raindrop formation from self-collection among cloud droplets, and thus further slowdown the loss of these small droplets from being collected by larger raindrops and allow more of them reach high altitudes, where they would eventually be collected by ice particles through riming, causing release of latent heat to enhance updraft.”

Regarding defining a weak or strong convective system in the case study, $3\text{ mm } 3\text{hr}^{-1}$ of the averaged rainfall could be used as a threshold. We have clarified this in the revised manuscript.

(3) The heating effect of fire aerosols seems too weak to have significant influence on circulation.

The temperature increase from aerosol absorption is not necessarily too weak because our analysis did identify clear change of vertical velocity owing to the aerosol heating effect. This seems also consistent with the analysis of Zhang et al. (2019). Indeed, should the heat flux generated by fires be incorporated in the model, the warming effects from biomass burning would be much stronger and also persist in nocturnal timeframe.

We have added sentences in Lines 522-527 of the revised manuscript as: “Based on our analysis, the temperature increase is mainly associated with the thermodynamic perturbation from the absorption of sunlight by fire aerosols. This seems also consistent with the analysis of Zhang et al. (2019). Indeed, should the heat flux generated by fires be incorporated in the model,

the warming effects from biomass burning would be much stronger and also persist in nocturnal timeframe.”

Here are also some specific comments:

1. Line 153: What is the time frequency of nudging?

The time frequency of nudging is every 6 hours. We have added this information in the revised manuscript.

2. Line 183: needless parenthesis

Modified.

3. Line 205: How and why were these convective systems selected? Why only three?

The selected cases in Section 3.2 are chosen randomly from different fire periods of the two study regions. We did not set any criteria initially when we chose these cases. All these points have been clarified in the revised manuscript (Lines 221-224):

”The selected cases are chosen randomly from the different fire periods of the two study regions. We did not set any criteria initially when we chose these cases. After we analyzed all cases, 3 mm 3hr⁻¹ was set as the threshold to distinguish weak and strong convections.”

These cases were used to discuss modeled characteristics of individual cases and make comparison between cases from different regions without considering their weights in the overall case-wise statistics. We have actually made effort to avoid leaving any impression about whether they are representative in their corresponding case population. The ensemble characteristics of each case population are defined by their case-wise statistics.

4. Line 233: Were the model results interpolated to the resolution of TRMM before doing the comparison?

The modeled rainfall in FFBB has been interpolated to the resolution of TRMM for the comparison in Figure 3. Figure 2a is also made by following this procedure. However, we have just realized that the original Fig. 2b was not made after modeled data being remapped into TRMM grids; therefore, we have reprocessed data and replotted Fig. 2b in the revised manuscript to be consistent with other figures. We appreciate the reviewer for pointing out this.

5. Line 260: Why only this example sounding is shown? You may compare with many other cases and even show a statistical comparison.

We choose this example sounding in the main text because we have cloud vertical structure from CALIPSO for the same case. We have now added the sounding comparison of other 5 cases in the supplement.

6. Line 275: Only one case captured by CALIPSO?

We have compared more than 50 modeled convections during the fire season and within the simulation domains. Specifically, for the six selected cases in case study, only one case was captured by CALIPSO. The others captured by CALIPSO are not among the cases in the case study (some are even out of our analyzed domains). This is the reason why we only discussed this case in our case study discussion. We have mentioned this point in Lines 302-304 of the revised manuscript.

7. Line 311-314: It is confusing. Aerosol impact on ice-phase microphysical processes is still considered in Morrison through the CCN effect. It is the IN effect of aerosol that is missed.

We thank the reviewer for indicating this. We have added “In our model configuration, fire aerosol can still affect ice process, however, through CCN effect rather than serving directly as ice nuclei.” into Lines 344-346 in the revised manuscript.

8. Line 315-321: More background information of these cases are necessary. You just simply saying that one case has weaker convective systems than other two. This is too ambiguous.

The reviewer’s comment is well taken. We have added the sounding profiles of all six cases in the supplement to present the environmental condition of each of these convections. We have also added a sentence of: “After we analyzed all cases, $3 \text{ mm } 3\text{hr}^{-1}$ was set as the threshold to distinguish weak and strong convections” into Lines 223-224 in the revised manuscript.

9. Line 454: The temperature increase seems too small. Is this significant? Maybe the difference is within the model simulating error range.

As we replied in the general comment (3), based on our analysis we believe this temperature increase is mainly associated with the thermodynamic perturbation from the absorption of sunlight by fire aerosols. It is also consistent with the analysis of Zhang et al. (2019). Again, should the heat flux generated by fires be incorporated in the model, the warming effects from biomass burning would be much stronger and also persist in nocturnal timeframe.

10. Line 455-457: No figure showing this conclusion. How much land breeze and surface convergence is weakened.

We have added Fig. 11 to demonstrate this conclusion in the revised manuscript.

Reference:

- Lin, J.C., Matsui, T., Pielke Sr., R.A., Kummerow, C., Effects of biomass-burning-derived aerosols on precipitation and clouds in the Amazon Basin: a satellite-based empirical study, *Journal of Geophysical Research: Atmospheres* **111**(2006).
- Wagner, A., Heinzeller, D., Wagner, S., Rummeler, T., Kunstmann, H., Explicit Convection and Scale-Aware Cumulus Parameterizations: High-Resolution Simulations over Areas of Different Topography in Germany, *Monthly Weather Review* **146**(2018), pp. 1925-1944.

Zhang, Y., Fan, J., Logan, T., Li, Z., Homeyer, C.R., Wildfire impact on environmental thermodynamics and severe convective storms, *Geophysical Research Letters* **0**(2019).

Responses to the Comments of the Anonymous Referee #3

We very much appreciate the constructive comments and suggestions from this reviewer. Our point-by-point responses to the reviewer's comments are as follows (the reviewer's comments are marked in *Italic font*).

Comments:

The authors attempt to investigate the fire aerosol-cloud-precipitation interactions by conducting modeling sensitivity studies. The performance of WRF-CHEM simulations were fully evaluated, and the responses of cloud microphysics and precipitation amount to fire aerosols were carefully quantified. However, I still have some minor issues about this work prior to its publication.

1. In the discussions in sections 3.1 and 3.2, it appears that the responses of cloud microphysics properties and precipitation to fire aerosols are sensitive to convection intensity of the systems selected for case studies, but the authors didn't show what are the criteria to determine the systems are convective weak. At least, some basic description about the selected convective systems should be provided so that the readership could have some sense about the convection strength of each system.

We thank the reviewer for pointing out this. The selected cases are chosen randomly from the difference fire periods of the two study regions. We did not set any criteria initially when we chose these cases. After we analyzed all cases, $3 \text{ mm } 3\text{hr}^{-1}$ was set as the threshold to distinguish weak and strong convections. We have clarified this in Lines 223-224 of the revised manuscript.

2. Related to point 1, is that possible to do statistical analysis of fire periods for weak and strong convective systems separately? Since the weak systems are more sensitive to fire aerosols, I would expect that there might be more significant differences in cloud properties or precipitation between fire aerosol case and non-fire aerosol case when looking at those weak systems.

The reviewer's suggestion is well taken. We have thus analyzed the weak against strong convections. Practically, however, it is difficult to directly use the same statistics in the case study to all the convections in different types, not mentioning the relativeness of the criterion for separating them when put all the cases together. Instead, we have performed statistics based on domain averages. Here again, the threshold of $3 \text{ mm } 3\text{hr}^{-1}$ for several selected cases is hard to apply to the domain wise statistical analysis, this is because that the domain-averaged rainfall in the statistical analysis is generally weaker than the averaged rainfall in the case study.

Therefore, we choose to use $1.25 \text{ mm } 3\text{hr}^{-1}$ of the domain-averaged rainfall to separate weak from strong convective systems. We find that the conclusions regarding differences of hydrometers and rainfall in the weak systems between the FF and FFBB experiments stay the same, and such differences are still not significant. We have added one paragraph in Sect. 3.3 for the statistical analysis for weak and strong convective systems during fire periods. In addition, Table S1 has been added to show average daily-rainfall of FFBB and FF for strong and weak convections during fire periods over the Sumatra region (r1) and Borneo region (r2), and Fig. S8 to indicate the mean hydrometeor differences in percentage between FFBB and FF.

3. Are the fire periods shown in Table 2 the time periods during which the fire aerosols are continuously emitted into atmosphere? I just want to make sure that the cloud systems selected for statistics of fire season are those which were indeed influenced by fire aerosols. That means the selected cloud systems for analysis concurrently occurred with fire events.

In our FFBB simulation, the fire aerosols were continuously emitted into the atmosphere. We present the time series of fire counts in the two study regions in Fig. S2.

4. Please add uncertainties of precipitation for each case in Figure 9.

We assume the figure referred by the reviewer was Fig. 10. The uncertainties have been added in Fig. 10 in the revised version of manuscript.

5. In section 3.4, the impacts of fire aerosols on local circulations like land/sea breeze are not evident. Some figures like the mean wind fields for fire aerosol and non-fire aerosol cases to show their difference would be helpful.

We thank the reviewer's comment. We have added a new figure (Fig. 11) in the revised manuscript to illustrate the sea breeze increase in FFBB during the daytime (20 LTC) and the land breeze decrease in FFBB during the night daytime (2 LTC).

1
2 **The Impacts of Biomass Burning Activities on Convective Systems in**
3 **the Maritime Continent**
4

5 Hsiang-He Lee^{1*}@ and Chien Wang^{1,2**}
6

7 ¹ Center for Environmental Sensing and Modeling, Singapore-MIT Alliance for Research
8 and Technology, Singapore

9 ² Center for Global Change Science, Massachusetts Institute of Technology, Cambridge,
10 MA, U.S.A.

11 *Now at Atmospheric, Earth, and Energy Division, Lawrence Livermore National
12 Laboratory, Livermore, CA, U.S.A.

13 **Now at Laboratoire d'Aerologie/CNRS/University of Toulouse, Toulouse, France
14
15
16
17
18
19

20 Submitted to
21 Atmospheric, Chemistry and Physics
22
23
24
25
26
27
28

29 July 2019
30

31 @Corresponding author address: Dr. Hsiang-He Lee, 7000 East Avenue, Livermore, CA,
32 94550, U.S.A.

33 E-mail: lee1061@llnl.gov

Deleted: .hsianghe@gmail.com

35 **Abstract**

36 Convective precipitation associated with Sumatra squall lines and diurnal rainfall
37 over Borneo is an important weather feature of the Maritime Continent in Southeast Asia.
38 Over the past few decades, biomass burning activities have been widespread during
39 summertime over this region, producing massive fire aerosols. These additional aerosols
40 brought to the atmosphere, besides influencing local radiation budget through directly
41 scattering and absorbing sunlight, can also act as cloud condensation nuclei or ice nuclei
42 to alter convective clouds and precipitation in the Maritime Continent via the so-called
43 aerosol indirect effects. Based on four-month simulations with or without biomass
44 burning aerosols conducted using the Weather Research and Forecasting model with
45 chemistry package (WRF-Chem), we have investigated the aerosol-cloud interactions
46 associated with the biomass burning aerosols in the Maritime Continent. Results from
47 selected cases of convective events have shown significant impacts of fire aerosols
48 specifically on the weak convections by increasing the quantities of hydrometeors and
49 rainfall in both Sumatra and Borneo regions. Statistical analysis over the fire season also
50 suggests that fire aerosols have impacts on the nocturnal convections associated with the
51 local anticyclonic circulation in the western Borneo and then weakened the nocturnal
52 rainfall intensity by about 9%. Such an effect is likely come from the near surface
53 heating by absorbing aerosols emitted from fires that could weaken land breezes and thus
54 the convergence of anticyclonic circulation.

Deleted: in

Deleted: amount either

Deleted: the

Deleted: or

Deleted: region

Deleted: substantial

Deleted: . In addition,

Deleted: from

Deleted: Therefore, the rainfall intensity of the nocturnal convections has been significantly decreased during the fire events.

55

56

68 **1 Introduction**

69 Biomass burning in Southeast Asia has become a serious environmental and societal
70 issue in the past decade due to its impact on local economy, air quality, and public health
71 (Miettinen et al., 2011; Kunii et al., 2002; Frankenberg et al., 2005; Crippa et al., 2016;
72 Lee et al., 2018). Abundant aerosols emitted from such fires not only cause
73 environmental issues but also affect regional weather and climate through the direct and
74 indirect effects of biomass burning aerosols (Grandey et al., 2016; Hodzic and Duvel,
75 2017; Jeong and Wang, 2010; Ramanathan and Carmichael, 2008; Taylor, 2010; Tosca et
76 al., 2013). Carbonaceous compounds such as black carbon (BC) in biomass burning
77 aerosols can reduce sunlight through both absorption and scattering to warm the
78 atmosphere while cool the Earth's surface (Fujii et al., 2014; Andreae and Gelencsér,
79 2006; Satheesh and Ramanathan, 2000; Ramanathan et al., 2001). Besides these direct
80 effects, biomass burning aerosols can act as cloud condensation nuclei or ice nuclei to
81 alter cloud microphysical structures and thus cloud radiation. Such "indirect effects" of
82 these aerosols on the climate are even more complicated due to various cloud and
83 meteorological conditions (Sekiguchi et al., 2003; Lin et al., 2013; Wu et al., 2013;
84 Grandey et al., 2016; Ramanathan et al., 2001; Wang, 2004).

85 For the Maritime Continent in Southeast Asia, convective precipitation associated
86 with the so-called Sumatra squall lines (SSL) and diurnal rainfall over Borneo is an
87 important weather feature (Lo and Orton, 2016; Ichikawa and Yasunari, 2006; Koh and
88 Teo, 2009; Yi and Lim, 2006; Wu et al., 2009). Convections of SSL are initially formed
89 in the northwestern side of Sumatra by the prevailing sea breezes from Indian Ocean and
90 the Sumatran mountain range, then propagate over the Malacca Strait affecting the Malay

91 Peninsula. Lo and Orton (2016) analyzed 22-year (1988 to 2009) ground-based Doppler
92 radar data and identified a total of 1337 squall lines in Singapore. They found that these
93 events with the diurnal cycle of rainfall most occur during either the summer monsoon
94 season (June-September) or the inter-monsoon periods (April-May and October-
95 November). Singapore, for example, experiences typically about 6~7 squall lines per
96 month during these periods. Oki and Musiaka (1994) analyzed the seasonal and diurnal
97 cycles of precipitation using rain gauge data and showed that large-scale low-level winds
98 are a critical modulating factor in the diurnal cycle the convective rainfall over Borneo
99 besides the general reason of land-sea contrast behind convective rainfall in the Maritime
100 Continent. Furthermore, Ichikawa and Yasunari (2006) used five years Tropical Rainfall
101 Measuring Mission (TRMM) precipitation radar (PR) data to investigate the role of the
102 low-level prevailing wind in modulating the diurnal cycle of rainfall over Borneo. They
103 found that the diurnal cycle is associated with intraseasonal variability in the large-scale
104 circulation pattern, with regimes associated with either low-level easterlies or westerlies
105 over the island.

106 Interestingly, frequent biomass burning activities coincide with vigorous convective
107 systems in the Maritime Continent, especially during the summer monsoon season (June-
108 September), and could thus produce aerosols to affect convections in the region.
109 Rosenfeld (1999) analyzed TRMM data and hypothesized that abundant biomass burning
110 aerosols could practically shut off warm rain processes in tropical convective clouds.
111 Compared to the adjacent tropical clouds in the cleaner air, clouds encountered with
112 smokes could grow to higher altitudes with rain suppressed, hypothetically due to the
113 reduction of coalescence efficiency of smaller cloud drops into raindrops. Recently,

114 using Weather Research and Forecasting model with Chemistry (WRF-Chem), Ge et al.
115 (2014) have studied the direct and semi-direct radiative effects of biomass burning
116 aerosols over the Maritime Continent and found the radiative effect of biomass burning
117 aerosols could alter planetary boundary layer (PBL) height, local winds (including sea
118 breeze), and cloud cover. However, relative coarse resolution (27 km) adopted in their
119 simulation would not be able to reveal more details about how biomass burning aerosols
120 affect convective clouds through modifying cloud microphysics processes. Whereas,
121 Hodzic and Duvel (2017) have conducted a 40-day simulation using WRF-Chem with a
122 convection-permitting scale (4 km) to study the fire aerosol-convection interaction during
123 boreal summer in 2009 near the central Borneo mountainous region. Their result
124 suggests that modifications of the cloud microphysics by biomass burning aerosols could
125 reduce shallow precipitation in the afternoon and lead to a warm PBL anomaly at sunset,
126 all lead to an enforcement of deep convection at night. However, they have also
127 indicated that the radiative processes of moderately absorbing aerosols tend to reduce
128 deep convection over most regions due to local surface cooling and atmosphere warming
129 that increase the static stability, hence suggesting the complexity of the interaction of
130 biomass burning aerosols and convective clouds in the Maritime Continent.

131 In this study, we aim to examine and quantify the impacts of biomass burning
132 aerosols on convective systems over two targeted regions for analyses: the northern
133 Sumatra and the western Borneo in the Maritime Continent. Our focus is on not only the
134 change of hydrometeors in the convective clouds but also the change of rainfall amount
135 and intensity in these regions. We firstly describe methodologies adopted in the study,
136 followed by the results and findings from our numerical simulations over the Maritime

137 Continent. We have selected three cases in each study region to perform detail analyses.
138 In addition, statistical analyses covering the entire modeled fire season for each of these
139 two regions have also been performed to provide more generalized pictures about the
140 effects of fire aerosol on convection. The last section summarizes and concludes our
141 work.

142 **2 Methodology**

143 **2.1 Model and emission inventories**

144 In order to simulate trace gases and particulates interactively with the meteorological
145 fields, the Weather Research and Forecasting model coupled with a chemistry module
146 (WRF-Chem, see Grell et al. (2005)) version 3.6.1 is used in this study. Within WRF-
147 Chem, the Regional Acid Deposition Model, version 2 (RADM2) photochemical
148 mechanism (Stockwell et al., 1997) coupled with the Modal Aerosol Dynamics Model for
149 Europe (MADE) as well as the Secondary Organic Aerosol Model (SORGAM)
150 (Ackermann et al., 1998; Schell et al., 2001) are included to simulate atmospheric
151 chemistry and anthropogenic aerosol evolutions. MADE/SORGAM uses a modal
152 approach to represent the aerosol size distribution and predicts mass and number
153 concentrations of three aerosol modes (Aiken, accumulation, and coarse).

154 To resolve the convective system in the Maritime Continent in our simulations, two
155 model domains with two-way nesting are designed. Here, Domain 1 (431×141 grid
156 cells) has a resolution of 25 km, while Domain 2 (561×591 grid cells) has a resolution
157 of 5 km (Fig. 1). Specifically, Domain 1 is positioned to include the tropical Indian
158 Ocean on its west half in order to capture the path of Madden-Julian Oscillation (MJO),

159 and in the meantime to have a northern boundary constrained within 23°N in latitude to
160 avoid potential numerical instability from the terrain of Tibetan Plateau. Domain 2 with
161 a finer resolution is positioned to cover the mainland Southeast Asia as well as the islands
162 of Sumatra and Borneo.

163 The National Center for Environment Prediction FiNaL (NCEP-FNL) reanalysis
164 data (National Centers for Environmental Prediction, 2000) are used to provide initial and
165 boundary meteorological conditions, and to perform four-dimensional data assimilation
166 (FDDA) to nudge model temperature, water vapor, and zonal and meridional wind speeds
167 above the planetary boundary layer (PBL) for Domain 1. The time frequency of nudging
168 is every 6 hrs. The Mellor-Yamada-Nakanishi-Niino level 2.5 (MYNN) (Nakanishi and
169 Niino, 2009) is chosen as the scheme for planetary boundary layer in this study. Other
170 physics schemes adopted in the simulations include Morrison two-moment microphysics
171 scheme (Morrison et al., 2009), RRTMG longwave and shortwave radiation schemes
172 (Mlawer et al., 1997; Iacono et al., 2008), Unified Noah land-surface scheme (Tewari et
173 al., 2004), and Grell-Freitas ensemble cumulus scheme (Grell and Freitas, 2014) (for
174 Domain 1 only). Owing to the main purpose of this study to reveal fire aerosol-
175 convection interaction through modeling a large quantity of convective systems
176 continually over a relatively long period, and the computational resource available to us
177 as well, we have adopted a 5 km horizontal resolution which excluding cumulus
178 parameterization scheme. Previous studies have shown that WRF model with a similar
179 resolution without convection parameterization can still capture many critical
180 characteristics of deep convection (Wagner et al., 2018). Our model evaluation,

181 especially through the comparison of modeled results with sounding profiles, has
182 demonstrated the same.

183 WRF-Chem needs emissions for gaseous and particulate precursors to drive its
184 simulations. For this purpose, we have used the Regional Emission inventory in ASia
185 (REAS) version 2.1 (Kurokawa et al., 2013). REAS includes emissions of most primary
186 air pollutants and greenhouse gases, covering each month from 2000 to 2008. In
187 addition, the Fire INventory from U.S. National Center for Atmospheric Research
188 (NCAR) version 1.5 (FINNv1.5) (Wiedinmyer et al., 2011) is also used in the study to
189 provide biomass burning emissions. FINNv1.5 classifies burnings of extratropical forest,
190 tropical forest (including peatland), savanna, and grassland. Fire heat fluxes for four
191 different types of fire are prescribed in WRF-Chem to calculate the plume height (rf.
192 Table 1 in Freitas et al. (2007)). For peatland fire, we have set its heat flux as 4.4 kW m⁻²,
193 which is the same as that of savanna burning and differs from that of the tropical forest
194 burning in 30 kW m⁻². The modified the plume rise algorithm in WRF-Chem to
195 specifically improve the representation of tropical peat fire has been described in Lee et
196 al. (2017). It is worth indicating that the heat flux from biomass burning is not
197 incorporated in thermodynamic equation of current WRF-Chem model. Note that the
198 current fire emission inventories could underestimate near surface fire aerosol
199 concentration by ignoring some of the characteristics of smoldering burning as well (Shi
200 et al., 2019).

201 The default chemical profiles of several species in the lateral boundary condition are
202 higher than their background concentrations in our study region and thus equivalent to
203 provide additional aerosol sources from boundaries. To prevent this, we have set NO,

Deleted: .

205 NO₂, SO₂, and all primary aerosol levels to zero at the lateral boundaries of Domain 1.
206 We have also adjusted the ozone profile used for lateral boundary condition based on the
207 World Meteorological Organization (WMO) Global Atmosphere Watch (GAW) station
208 in Bukit Kototabang, Indonesia (Lee et al., 2019).

Deleted: (Lee et al. (2019))

209 2.2 Numerical experiment design

210 Two numerical simulations, both included anthropogenic emissions (mainly fossil
211 fuel emissions) while either with and without the biomass burning emissions (labeled as
212 FFBB and FF, respectively), have been conducted to investigate the impacts of biomass
213 burning aerosols on convective systems in the Maritime Continent through both direct
214 and indirect effects. Our study focuses on the fire season from June to September of
215 2008. Therefore, the simulations start from 1 May of 2008 and last for five months. The
216 first month is used as a spin-up period. Among the years with available emission data,
217 both emission amount of biomass burning and total precipitation in 2008 approximate
218 their ensemble mean or represent an average condition (Fig. S1). Nevertheless,
219 interannual variation of biomass burning emissions alongside precipitation in the studies
220 regions do exist (Lee et al., 2017; Lee et al., 2018), and the influence of such variation on
221 the effects of fire aerosol on convection should be addressed in future studies.

Deleted: include

Deleted: .

222 2.3 Analysis methods

223 The primary target of this study is the convective systems associated with Sumatra
224 squall lines and diurnal rainfall over Borneo. Thus, our analyses mainly focus on the
225 convections over two specific regions: the Sumatra region (r1 in Fig. 1) and the Borneo
226 region (r2 in Fig. 1). The area coverage of the Sumatra region (r1) is from 97° to 103° E

230 in longitude and 0° to 6° N in latitude, while the area coverage of the Borneo region (r2)
231 is from 109° to 115° E in longitude and 1° S to 5° N in latitude.

232 To examine the impacts of fire aerosols on cloud formation and rainfall intensity as
233 well as amount, we have selected three convective systems each for the two focused
234 regions to perform an in-depth case study. We first trace the path of individual
235 convections and focus the analyses on the specific area of each of these convective
236 systems to identify the impacts of fire aerosols. Table 1 shows the selected cases in the
237 Sumatra region (r1) and the Borneo region (r2). The selected cases are chosen randomly
238 from different fire periods of the two study regions. We did not set any criteria initially
239 when we chose these cases. After we analyzed all cases, 3 mm 3hr⁻¹ was set as the
240 threshold to distinguish weak and strong convections.

241 The consequent analyses are then focused on the fire-season-wise statistics of
242 convections for each study region. Table 2 and Fig. S2 show the fire periods in the two
243 study regions. There are total of 54 convective systems simulated during the fire periods
244 in the Sumatra region (r1) and 35 convective systems in the Borneo region (r2).

245 The statistical quantities used in this study follows Wang (2005) to estimate the
246 mean value over a specific region (e.g., r1 or r2). The cloud area mean quantities are
247 defined as a function of output time step (t) by the following equation:

$$248 \quad c^{area}(t) = \frac{1}{N(t)} \sum_{\substack{q > q_{min} \\ n > n_{min}}} c(x, y, z, t). \quad (1)$$

249 Here c is a given quantity (e.g., cloud water mass). Eq. (1) only applies to the grid points
250 where both the mass concentration q and number concentration n of a hydrometeor
251 exceed their given minima. The total number of these grid points at a given output time
252 step t is represented by $N(t)$. The cloud area mean quantities are used to present the

Deleted: shows

254 average quantities of a given variable at a given output time step. Note that the cloud
255 area mean quantities only apply to hydrometeors. For rainfall, the analyzed quantities are
256 spatial averages over a specific area of the convective system for case study or over the
257 entire study region for longer-term statistic estimate.

258 **3 Results**

259 **3.1 Model evaluation**

260 **3.1.1 Precipitation**

261 The satellite-retrieved precipitation of the Tropical Rainfall Measuring Mission
262 (TRMM) 3B42 3hrly (V7) dataset (Huffman et al., 2007) is used in this study to evaluate
263 simulated rainfall. Figure 2a and 2b show the Hovmöller plots of daily TRMM and
264 FFBB precipitation from 1 June 2008 to 30 September 2008, respectively. Compared to
265 the satellite-retrieved data, the model has captured all the major rainfall events in the two
266 analysis regions (Fig. 3). In addition, because of its higher spatial resolution than
267 TRMM, the model produces more light rain events. Nevertheless, as indicated in our
268 previous study (Lee et al., 2017), a wet bias of the model is evident and mainly comes
269 from water vapor nudging in data assimilation (FDDA). As a result, the daily average
270 rainfall in FFBB over the Sumatra region ($r1$) is 11.05 ± 5.90 mm day⁻¹ from 1 June 2008
271 to 30 September 2008, higher than that of 7.21 ± 5.54 mm day⁻¹ derived from TRMM
272 retrieval. The wet bias also exists in the modeling results in the Borneo region ($r2$),
273 where daily average rainfall there is 15.40 ± 8.49 mm day⁻¹ in FFBB and only 9.56 ± 7.20
274 mm day⁻¹ in TRMM. For the simulated rainfall in FFBB, the temporal correlation with
275 TRMM is 0.44 in the Sumatra region ($r1$) and 0.64 in the Borneo region ($r2$).

276 **3.1.2 Aerosol optical depth (AOD)**

277 Because of limited ground-based observational data of aerosols, we use Aerosol
278 Optical Depth (AOD) from the level-3 Moderate Resolution Imaging Spectroradiometer
279 (MODIS) gridded atmosphere monthly global joint product (MOD08_M3;
280 http://dx.doi.org/10.5067/MODIS/MOD08_M3.061) to evaluate modeled aerosol spatial
281 distribution and relative concentration. Figure 4a shows MODIS monthly AOD in
282 Southeast Asia in September 2008. High AOD occurs in the southern part of Sumatra
283 and the southwestern part of Borneo. Compared to the MODIS retrieval, the modeled
284 AOD in FFBB has similar spatial distribution but a higher value (Fig. 4b). It is because a
285 high spatiotemporal resolution in our simulation enables the model to capture episodic
286 fire events better. In contrast, FF simulation produces much lower AOD values than
287 those of MODIS and FFBB, thus suggesting biomass burning aerosols make a substantial
288 fraction in atmospheric AOD during burning seasons.

289 **3.1.3 Sounding profiles**

290 We have used multiple weather sounding profiles measured in Bintulu Airport,
291 Malaysia (113.03° E, 3.20° N), provided by University of Wyoming
292 (<http://weather.uwyo.edu/upperair/sounding.html>). An example for detailed summary is
293 a case at 12 UTC on 22 September 2008 (Fig. 5a). This sounding provides information
294 of atmospheric state (e.g., vertical distributions of pressure, temperature, wind speed,
295 wind direction, and humidity) coinciding with one of our selected case study (r2c3) of
296 diurnal convective rainfall in Borneo. Compared to the observed sounding data, the
297 FFBB simulation has produced similar temperature and wind profiles and well captured

298 the low-level and high-level wind speeds and wind directions (Fig. 5a versus 5b). It also
299 well predicts several key indexes of convection: temperature and pressure of the Lifted
300 Condensation Level (LCL) simulated in FFBB are 296.2 K and 955 hPa, respectively,
301 which are close to the values of 296.2 K in temperature and 960.7 hPa in pressure derived
302 from the observed sounding data. The model predicts 3049 J of Convective Available
303 Potential Energy (CAPE), while 2031 J of CAPE is estimated in the observed sounding
304 data. Besides this 22 September 2008 case, the model has also captured major features of
305 observed profiles for all the other cases selected in our analyses, shown in Fig. S3~S7.

Deleted: .

306 **3.1.4 Cloud vertical structure**

307 The Cloud-Aerosol Lidar and Infrared Pathfinder Satellite Observation (CALIPSO)
308 provides information of the vertical structure of clouds on its path around the globe
309 (https://www-calipso.larc.nasa.gov/products/lidar/browse_images/production/), including
310 that of one of our cases (r2c3) of diurnal convective rainfall in Borneo on 22 September,
311 2008 (Fig. 6a). For this case, CALIPSO shows the vertical structure of a convective
312 system over Borneo along with high PM_{2.5} concentration near the surface (yellowish
313 color near the surface), implying a potential impact of biomass burning aerosols on
314 convective clouds. It can be seen that the FFBB simulations well captures the vertical
315 structure of convective clouds as well as the near-surface aerosol layers, including their
316 vertical extension (Fig. 6c versus 6a). With the comparison of FF simulation, we are able
317 to identify the biomass burning origin of these aerosols near the surface. It is worth to
318 indicate that we have compared more than 50 modeled convections during the fire season
319 and within the simulation domains. However, the others captured by CALIPSO are

Deleted: 22

§22 either not among the selected cases or are mostly out of our analyzed domains, so we did
§23 not have further discussion here.

324 **3.2 Analyses of selected cases in two study regions**

325 **3.2.1 The Sumatra region (r1)**

326 The three selected cases in r1 or the Sumatra region (r1c1, r1c2 and r1c3) all
327 occurred in the afternoon (2 PM or 5 PM local time) and lasted less than 24 hours (Table
§28 1). The sounding profile of three cases show quite similar to the environmental profiles
§29 (Fig. S3~S5). Most fire aerosols in this study region were initially emitted from the
330 central and south Sumatra then transported along with southwesterly winds to encounter
331 convections in the northern Sumatra. Compared to the result of FF, PM_{2.5} concentration
332 in FFBB can be 6~12 times higher in the Sumatra region (r1) in these selected cases (Fig.
333 7).

334 Aerosols from biomass burning in FFBB add 2~3 times more cloud droplet number
335 concentration and 8~20% higher cloud water mass compared to the results in FF (Table
336 2). The mean radius of cloud droplets in FFBB is about 6~7 μm, clearly smaller than that
337 in FF (10~11 μm). Smaller cloud droplet in FFBB reduces the efficiency of
338 autoconversion, and further decreases rain water mass and raindrop number
339 concentration. Hence, raindrop number concentration in FFBB is 40~50% lower than
340 that in FF among our selected cases in r1 (Table 3). However, besides autoconversion,
341 rain water mass is also affected by other microphysics processes. Larger raindrops
§42 combining with smaller cloud droplets in FFBB can enhance the efficiency of cloud
§43 droplet collection by rain and thus increase rain water mass but cause no change to the

Deleted: increase

Deleted: produce higher

346 number of raindrops, possibly compensating the decrease of rain water mass resulted
347 from a lowered autoconversion. Overall, rain water mass decreases 15% in the case of
348 r1c2 and 10% in the case of r1c3, respectively. Compared to the cases of r1c2 and r1c3,
349 the case of r1c1 is a relatively weak convective system, based on a threshold of ~3 mm
350 3hr⁻¹ of the averaged rainfall in FF (Table 4). After introducing fire aerosols, the mass
351 concentration of snow and graupel in this case increases 62% and 48%, respectively.
352 Melting snow and graupel in the lower atmosphere results in a significant increase of rain
353 water mass concentration by 49%. Thus, total hydrometeor mass is increased by 36% in
354 FFBB from that in FF. Our result is consistent with that of Lin et al. (2006), which
355 suggested that biomass burning aerosols could invigorate convection and then increase
356 precipitation based on satellite observations. The aerosol invigoration effect is referred to
357 such a hypothetic process that increasing number of smaller cloud droplets due to higher
358 aerosol concentration would reduce the efficiency of raindrop formation from self-
359 collection among cloud droplets, and thus further slowdown the loss of these small
360 droplets from being collected by larger raindrops and allow more of them reach high
361 altitudes, where they would eventually collected by ice particles through riming, causing
362 release of latent heat to enhance updraft. Note that the “aerosol-aware” microphysics
363 scheme in WRF-Chem only applies to the warm cloud process (Morrison et al., 2005;
364 Morrison et al., 2009); therefore, ice nucleation is parameterized of ambiance temperature
365 only regardless of the aerosol concentration. In our model configuration, fire aerosol can
366 still affect ice process, however, through CCN effect rather than serving directly as ice
367 nuclei.

Deleted: .

369 In the FF simulations, the convective system in the case of r1c2 and r1c3 is stronger
370 than the system in the case of r1c1, and the average rainfall of r1c2 and r1c3 is also
371 higher than the rainfall of r1c1 (Table 4). Adding fire aerosols in FFBB does not
372 substantially change the average rainfall in r1c2 and r1c3 (+3% and -8%, respectively;
373 Table 4). However, in the relatively weak convective system of r1c1, adding fire
374 aerosols significantly increases the mean rainfall amount by 106% ($1.33 \pm 0.47 \text{ mm } 3\text{hr}^{-1}$
375 in FF versus $2.74 \pm 1.21 \text{ mm } 3\text{hr}^{-1}$ in FFBB).

376 3.2.2 The Borneo region (r2)

377 The three selected cases in r2 (r2c1, r2c2, and r2c3) also occurred during the summer
378 monsoon season when active biomass burning events existed in the west Borneo. In
379 these cases, fire aerosols were transported to the north and northeast by the southeasterly
380 and southwesterly winds. Because of the proximity of fire emissions, the $\text{PM}_{2.5}$
381 concentration in FFBB can be 24 times higher than that in FF in the Borneo region (r2) in
382 these selected cases (Fig. 7).

383 The modeled results demonstrate the substantial impacts of fire aerosols on both
384 ambient aerosol concentration and cloud droplet number concentration. $\text{PM}_{2.5}$
385 concentration in FFBB is drastically higher than that in FF with the highest increase
386 appears in the case of r2c1 at 4940%, more than doubled the values of r2c2 (2402%) and
387 r2c3 (2422%). The increase in cloud droplet number concentration in the case of r2c1
388 (703%) is also substantially higher than those in r2c2 (337%) and r2c3 (409%) (Table 2).

389 The mean radius of cloud droplets in FFBB is about 6~7 μm , which is significantly
390 smaller than that in FF (10~11 μm). The mean cloud droplet radii in FF and FFBB in r2

Deleted: substantially

392 are similar to the results in r1. On the other hand, the increase of cloud water mass due to
393 fire aerosols is not so dramatic in all these cases, only about 8%~27% higher than that in
394 the FF simulations (Table 3). As discussed above, rain number concentration in FFBB
395 over the Borneo region (r2) is lower than that in FF, similar to the cases in r1, likely due
396 to the low efficiency of autoconversion induced by the presence of a large quantity of
397 smaller cloud droplets. Rain water mass of FFBB in the r2c1 case is decreased by about
398 6% due to fire aerosols, which is similar to the results in the r1c2 and r1c3 cases over the
399 Sumatra region (Table 3). However, interestingly, rain water and snow mass are both
400 increased in FFBB by 64% and 69% in r2c2 and by 19% and 60% in r2c3, respectively
401 (Table 3). The cases of r2c2 and r2c3 are relatively weak convective systems, similar to
402 the case of r1c1. Again, it is based on based on a threshold of $\sim 3 \text{ mm } 3\text{hr}^{-1}$ of the
403 averaged rainfall in FF (Table 4). Our results show that fire aerosols have substantial
404 impacts on cold cloud processes in the weak convective systems. Overall, total
405 hydrometeor mass concentration in FFBB have increased 47% in r2c2 and 13% in r2c3.

Deleted: substantially

406 The changes of rainfall amount due to fire aerosols in r2 are similar to the cases in r1.
407 For the strong convection case of r2c1, adding fire aerosols in the FFBB simulation
408 decreases the total rainfall amount by 18%. However, in the weak convection cases of
409 r2c2 and r2c3, adding fire aerosols would double the rainfall amount (Table 4).
410 Compared to the results in FF, rainfall intensity is persistently higher in FFBB during the
411 convection life cycle in those weak convection cases. Nighttime rainfall intensity in
412 FFBB, especially, is much higher than the rainfall intensity in FF. Therefore, as shown
413 by our results, fire aerosols appear to have more substantial impacts on the quantities of

415 hydrometeors and rainfall of the weak convection cases in both Sumatra region (r1) and
416 Borneo region (r2).

417 Our results show that fire aerosols tend to invigorate weak convection but suppress
418 deep convection in both Sumatra region (r1) and Borneo region (r2). As mentioned
419 before, increasing the number of smaller cloud droplets due to higher aerosol
420 concentration resulted from fire would reduce the efficiency of raindrop formation
421 through the warm-rain processes, thus allowing more cloud droplets reach high altitudes
422 to be eventually collected by ice particles through riming, causing release of latent heat to
423 invigorate updraft while enhancing precipitation through melting of fallen ice particles
424 (Wang, 2005). These processes appear to be more effective to weak convections than
425 deep convections and were in fact well-simulated in the former cases. The results are
426 also consistent with some previous observation-based studies (Jiang et al., 2018; Zhao et
427 al., 2018). Jiang et al. (2018) and Zhao et al. (2018) both concluded that an increase of
428 fire aerosols generally reduces cloud optical thickness of deep convection while Zhao et
429 al. (2018) further showed that fire aerosols tend to invigorate weak convection for small-
430 to-moderate aerosol loadings.

431 **3.3 Fire-season statistics of convections in two study regions**

432 Statistics covering the entire simulated fire season (~4 months) for each study region
433 have been derived to provide trend/tendency information regarding several aspects of the
434 impact of fire aerosols on convections. In our simulations, PM_{2.5} concentration in FF
435 during the fire periods, which can be regarded as the background value for FFBB
436 simulation before adding fire aerosols, is $1.36 \pm 0.19 \mu\text{g m}^{-3}$ in r1 and $0.56 \pm 0.09 \mu\text{g m}^{-3}$ in

437 r2. In comparison, $PM_{2.5}$ concentration in FFBB is $11.37 \pm 10.41 \mu\text{g m}^{-3}$ in r1 and
438 $10.07 \pm 7.73 \mu\text{g m}^{-3}$ in r2. Note that unlike in some other studies where the control
439 simulations use constant aerosol concentrations, fire aerosol concentrations in our
440 simulations can vary in responses to changes in fire emissions, or aerosol removal by rain
441 scavenging due to precipitation change caused by fire aerosols themselves. Hence, the
442 processes included in our simulations are closer to reality, and the results could better
443 reflect the nature of fire aerosol-convection interaction in the Maritime Continent.

444 Averaged through the entire modeled fire periods, cloud water mass (Q_c), cloud
445 droplet number concentration (Q_{nc}), and rain drop number concentration (Q_{nr}) in FFBB
446 differ substantially from those in FF, demonstrating the influence of fire aerosols. Figure
447 8 shows that adding fire aerosols in FFBB would increase Q_c by 14% and Q_{nc} by 226%
448 in r1, and Q_c by 18% and Q_{nc} by 349% in r2. Another pronounced change in response to
449 adding fire aerosols is a decrease in Q_{nr} by 44% in r1 and 47% in r2. Although an
450 increase in snow mass (Q_s) and graupel mass (Q_g) and a decrease in rain water mass (Q_r)
451 after adding fire aerosols, the uncertainty of these hydrometeor changes is large.

452 In Sect. 3.2, we have discussed the significant rainfall increase occurred in the weak
453 convective systems after adding fire aerosols, due to aerosol invigoration effect. On one
454 hand, regardless the strength of convection, the mean 3-hourly rainfall during the fire
455 periods is $1.06 \pm 0.85 \text{ mm}$ in FF and $1.09 \pm 0.86 \text{ mm}$ in FFBB over the Sumatra region (r1),
456 and statistically it does not change, significantly in responding to fire aerosols. The
457 rainfall difference in the Borneo region (r2) between FF and FFBB is also insignificant
458 ($1.32 \pm 1.20 \text{ mm 3hrs}^{-1}$ in FF versus $1.35 \pm 1.14 \text{ mm 3hrs}^{-1}$ in FFBB). On the other hand,
459 we have found that the impacts of fire aerosols appear in several other rainfall patterns.

Deleted: . Here we use the fire-season statistics

Deleted: further this discussion. Regardless

Deleted: convective precipitation

Deleted: 3hrs^{-1}

Deleted: 3hrs^{-1}

Deleted: .

466 For instance, the daily maximum and minimum rainfalls display clear differences
467 between the FFBB and FF simulations, specifically in r2 rather than in r1 (Fig. 9). While
468 for r1, the impacts of fire aerosol are reflected in event-wise statistics, e.g., higher event-
469 wise maximum and minimum rainfall intensity in FFBB than in FF, identified in 30 out
470 of 54 convective events in total. These are mostly weak convective events in r1.
471 Interestingly, somewhat opposite to the rainfall statistics in r1, the intensity of event-wise
472 maximum and minimum rainfall in r2 is higher in FF than in FFBB. The daily rainfall
473 peak of 3-hr rainfall in r1 is mostly less than 3 mm; in comparison, one-third of
474 convective events in r2 have daily maximum 3-hr rainfall exceeding 3 mm (Fig. 9c),
475 suggesting that the convective systems in r2 tend to develop stronger than in r1 and the
476 fire aerosols significantly suppress the maximum rainfall intensity of strong convections
477 in r1. We roughly used $1.25 \text{ mm } 3\text{hr}^{-1}$ of the domain-averaged rainfall to classify weak
478 and strong convective systems. We find that the conclusions regarding differences of
479 hydrometers and rainfall in the weak systems between the FF and FFBB experiments stay
480 the same, and such differences are still not that significant in both regions (Table S1 and
481 Fig. S8).

482 We have categorized the maximum rainfall based on its values in the afternoon and
483 midnight. We find that those heavy maximum rainfalls in r2 tend to occur in the
484 midnight (Fig. 9c) associated with the anticyclonic circulation formed in the western
485 Borneo induced by southeasterly winds from the Southern latitude turn northeastward
486 along the west coast of Borneo, owing to the terrain of Borneo Island and the sea breezes
487 from the South China Sea. The vortex produced by such a circulation leads to strong
488 updraft and then strong convection. Note that this anticyclonic circulation is different

Deleted: On the other hand, based on the diurnal rainfall pattern in two study regions, we notice that daily maximum and minimum rainfall show apparent differences between the FFBB and FF simulations in r2, while such differences are rather small in r1 (Fig. 9). The maximum or minimum rainfall intensity in the two simulations are closely aligned with the 1:1 line in Fig. 9a and 9b. However, when looking into each of the 54 convective events in r1, there are 30 events where the model predicted higher maximum and minimum rainfall intensity in FFBB than in FF. These are mostly weak convective events. ¶
Additionally, and somewhat opposite to the rainfall statistics in r1, the intensity of maximum and minimum rainfall in r2 is higher in FF than in FFBB. The daily rainfall peak in r1 is mostly less than $3 \text{ mm } 3\text{hrs}^{-1}$; in comparison, one-third of convective events in r2 have daily maximum rainfall exceeding $3 \text{ mm } 3\text{hrs}^{-1}$

506 from the Borneo vortex, the latter appears as a persistent feature of the boreal winter
507 climatology and is related to the northeasterly from the South China Sea and cold surge
508 events (Chang et al., 1983; Chang et al., 2005).

509 The low-level wind pattern of Borneo convections is similar to the westerly regime,
510 especially the weak westerly (WW) regime identified by Ichikawa and Yasunari (2006).
511 According to their analysis, the WW regime tends to occur in boreal summer. Its
512 composites include an anticyclonic feature with the weak wind field over the Borneo
513 Island. The deep convective storms developed in the WW regime tend to stay close to
514 the west coast associated with the lower-level convergence enhanced by the prevailing
515 wind and local circulations around there, resulting in localized rainfall over the offshore
516 region of the west coast. Based on our simulations, the onset of convection occurs in the
517 afternoon over the western mountain range of Borneo. These storms would consequently
518 evolve into widespread shallow storms in the evening over the western part of the island.
519 The maximum rainfall appears on the west coast because of a local westward propagating
520 rainfall system that develops around midnight or early morning.

521 The comparison of the maximum rainfall between FF and FFBB in Fig. 9 shows that
522 fire aerosols tend to reduce the maximum rainfall, especially for high-intensity rainfall
523 events. In other words, fire aerosols have substantial impacts on the nocturnal
524 convections, which are associated with the local anticyclonic circulation in the western
525 Borneo. This effect on nocturnal convections in the western Borneo by fire aerosols will
526 be discussed further in the next section.

527 **3.4 The impact of biomass burning activities on nocturnal**
528 **convections in the Borneo region**

529 To further analyze the effects of fire aerosols on nocturnal convections, we have
530 categorized convective events into nocturnal convections (NC) and non-nocturnal
531 convections (non-NC), based on whether the maximum rainfall occurs from midnight to
532 early morning or in the time frame from late afternoon to evening. Figure 10 shows the
533 diurnal time series of precipitation averaged over the Borneo region (r_2) in FF and FFBB.
534 Again, 3-hour-mean rainfalls of nocturnal convections are higher than those of non-
535 nocturnal convections in both simulations, and fire aerosols weaken the maximum
536 nocturnal rainfall intensity about 9%.

Deleted: .

537 Nocturnal convections tend to stay close to the west coast associated with a lower-
538 level convergence enhanced by the prevailing wind and local circulations mainly related
539 to the land breezes from inland of the western Borneo. The strong convergence near the
540 surface over the offshore region of the west coast causes the weak westerly monsoon
541 windflaws and local land breezes to merge during the nighttime. However, during the
542 fire periods, the daytime absorption of fire aerosols (e.g., black carbon) can cause an
543 atmospheric warming (even without fire generated heating flux being incorporated in the
544 model). This could increase near surface air temperature, weaken land breezes and thus
545 surface convergence, (Fig. 11b). As a result, the nocturnal convections in FFBB cannot
546 develop as strong as those in FF. On the other hand, both nocturnal and non-nocturnal
547 convections are initiated over the western mountain range under a prevailing wind of the
548 sea breezes from the South China Sea. The increases of near surface temperature owing

Deleted: .

551 to the fire aerosols can enhance this prevailing wind from the ocean (Fig. 11a) and thus
552 lead to a higher convective rainfall in FFBB during the onset stage of the nocturnal
553 convections as well as non-nocturnal convections.

554 Diurnal evolution of vertical profiles clearly indicates that mass mixing ratio of total
555 hydrometeors, temperature, and vertical velocity differ in both daytime and nighttime

556 between FF and FFBB for those nocturnal convections (Fig. 12). The differences of near
557 surface temperature between FF and FFBB are more pronounced during the period after

558 sunset (Fig. 12d). The differences of near surface temperature mainly happen over land,
559 and the higher near surface temperature in FFBB weakens the land breezes and near

560 surface convergence along the coast. Starting from late afternoon, (about 5 PM local
561 time), vertical velocity increases with time until sunrise next day in both simulations (Fig.

562 12e) due to the convergence of the monsoon windflaws and local land breezes during the
563 nighttime, and this matches very well with that of mass mixing ratio of total

564 hydrometeors (Fig. 12a and 12e). Noticeably, the main differences in vertical velocity
565 and hydrometeor mass mixing ratio between FFBB and FF also start to become evident

566 after entering the evening. Because of the weaker convergence near the surface in FFBB,
567 the differences in vertical velocity at the higher altitude between FFBB and FF peaks in

568 the nighttime. The temperature increase from aerosol absorption seems small (please
569 note that the direct heating from fire is not included in the WRF fire plume model) but we

570 do see the change of vertical velocity owing to the aerosol heating effect. Based on our
571 analysis, the temperature increase is mainly associated with the thermodynamic

572 perturbation from the absorption of sunlight by fire aerosols. This seems also consistent
573 with the analysis of Zhang et al. (2019). Indeed, should the heat flux generated by fires

Deleted: 11

Deleted: 11d

Deleted: 11e

Deleted: 11a

Deleted: 11e

Deleted: ¶
It should be indicated that if the heat flux generated by fires was incorporated in the model, the warming effects from biomass burning would be even stronger and could persist in nocturnal timeframe as demonstrated in

Deleted: However, this would likely be more effective for open fire regime. For most of peat fires, burning is largely proceeded underground. Based on our significantly reduced heat flux for the peat fires as discussed in Sect. 2.1, if the heat flux was incorporated in the model, such fires would not increase surface temperature by 4-5 °C as suggested for the tropical (open) fire cases in Zhang et al. (2019)...

591 be incorporated in the model, the warming effects from biomass burning would be much
592 stronger and also persist in nocturnal timeframe.

593 As a summary, the schematics shown in Fig. 13 illustrate the impact of biomass
594 burning activities on nocturnal convections in the Borneo region. In the daytime, under
595 the prevailing wind of sea breezes from the South China Sea, convections develop over
596 the western mountain range. Because near surface heating from the absorption of
597 sunlight by fire aerosols could enhance the prevailing wind from the ocean, convective
598 rainfall becomes higher at the onset stage of the nocturnal convections (still in daytime)
599 due to biomass burning activities (Fig. 13b). In the nighttime, convection moves to the
600 offshore region of the western Borneo. The strong convergences near the surface merge
601 the weak westerly monsoon windflaws with local nighttime land breezes to form an
602 anticyclonic circulation (Fig. 13c). During the fire periods, the daytime near surface
603 warming by fire aerosols could also further weaken land breezes and surface
604 convergence. Hence, the nocturnal convections during fire events would not develop as
605 strong as in days without fires (Fig. 13d versus 13c).

606 4 Summary

607 By comparing WRF-Chem modeling results include or exclude biomass burning
608 emissions (FFBB versus FF), we have identified certain detailed impacts of fire aerosols
609 on convective events within two study regions in the Maritime Continent during a four-
610 month period (June 2008 ~ September 2008). In total, 54 convective systems in the
611 Sumatra region and 35 convective systems in the Borneo region have been simulated.
612 Three convective events of each study region have been selected for in-depth

Deleted: 12

Deleted: 12b

Deleted: 12c

Deleted: 12d

Deleted: 12c

618 investigation. In addition, statistical analyses have been performed throughout the entire
619 simulation period for each region. We have focused our analyses on two rainfall
620 features: 1) convective precipitation associated with Sumatra squall lines, and 2) diurnal
621 rainfall over the western Borneo.

622 We find that fire aerosols lead to the increase of cloud water mass and cloud droplet
623 number concentration among all analyzed cases while a substantial reduction of rain drop
624 number concentration. Influences of fire aerosols on other hydrometeors vary from case
625 to case. Specifically, our results show that fire aerosols can significantly change the
626 quantities of hydrometeors, particularly those involved in cold cloud processes and
627 rainfall of weak convections in either the Sumatra region or the Borneo region. Rainfall
628 intensity is higher in FFBB during the entire convection life cycle in those weak
629 convection cases, and the nighttime rainfall intensity in FFBB is significantly higher than
630 that in FF.

631 Statistics performed throughout the entire modeled fire season shows that the fire
632 aerosols only cause a nearly negligible change (2-3%) to the total rainfall of convective
633 systems in both study regions. On the other hand, we notice that fire aerosols can still
634 alter daily maximum and minimum rainfall in some cases, for example, fire aerosols lead
635 to the increase of maximum and minimum rainfall intensity in 30 weak convective events
636 in the Sumatra region.

637 In the Borneo region, biomass burning activities mainly affect the rainfall intensity
638 of nocturnal convection. Because near surface heating from the absorption of fire
639 aerosols can enhance the prevailing wind from the ocean (sea breeze) during the daytime,
640 the convective rainfall over the western mountain range is higher during the onset stage

641 of the nocturnal convections. In the nighttime, the consequence of the above
642 thermodynamic perturbation by absorbing fire aerosols can further weaken land breeze
643 and surface convergence. Hence, the rainfall intensity of nocturnal convections under the
644 influence of fire aerosols would become weaker by about 9%.

Deleted: .

645 This study has demonstrated how biomass burning activities could affect convective
646 systems in the Maritime Continent by altering cloud microphysics and dynamics. We
647 find the biomass burning activities significantly change the diurnal rainfall intensity,
648 especially those low-level wind patterns associated with the weak westerly (WW) regime
649 as suggested by Ichikawa and Yasunari (2006). Our results show that neither a single
650 case study nor a simple statistical summary applied to overall model simulation period
651 without in-depth analyses could reveal the impact of biomass burning aerosols on
652 convections under different windflow regimes.

653 **Data availability**

654 FINNv1.5 emission data are publicly available from
655 <http://bai.acom.uar.edu/Data/fire/>. REAS emission data can be downloaded from
656 <https://www.nies.go.jp/REAS/>. TRMM data can be obtained from
657 <https://pmm.nasa.gov/data-access/downloads/trmm>. AOD from MODIS can be
658 obtained from http://dx.doi.org/10.5067/MODIS/MOD08_M3.061. Sounding profiles
659 are publicly available on <http://weather.uwyo.edu/upperair/sounding.html>. WRF-Chem
660 simulated data are available upon request from Hsiang-He Lee (lee1061@llnl.gov).

662 **Author contribution**

663 H.-H. L. and C. W. designed the experiments and H.-H. L. carried them out. H.-H.
664 L. configured the simulations and analyzed the results. H.-H. L. and C. W. wrote the
665 manuscript.

666 **Acknowledgments**

667 This research was supported by the National Research Foundation Singapore through
668 the Singapore-MIT Alliance for Research and Technology, the interdisciplinary research
669 program of Center for Environmental Sensing and Modeling. It was also supported by
670 the U.S. National Science Foundation (AGS-1339264) and L'Agence National de la
671 Recherche (ANR) of France through the Make-Our-Planet-Great-Again Initiative, ANR-
672 18-MPGA-003 EUROACE. The authors would like to acknowledge NCEP-FNL and
673 NCAR FINN working groups for releasing their data to the research communities; and
674 the NCAR WRF developing team for providing the numerical model for this study. The
675 computational work for this article was performed on resources of the National
676 Supercomputing Centre, Singapore (<https://www.nscg.sg>).

677

678

679

680

681

682 **Reference:**

- 683 [Ackermann, I. J., Hass, H., Memmesheimer, M., Ebel, A., Binkowski, F. S., and](#)
684 [Shankar, U.: Modal aerosol dynamics model for Europe: development and first](#)
685 [applications, *Atmospheric Environment*, 32, 2981-2999,](#)
686 [http://dx.doi.org/10.1016/S1352-2310\(98\)00006-5](http://dx.doi.org/10.1016/S1352-2310(98)00006-5), 1998.
- 687 [Andreae, M. O., and Gelencsér, A.: Black carbon or brown carbon? The nature of](#)
688 [light-absorbing carbonaceous aerosols, *Atmos. Chem. Phys.*, 6, 3131-3148,](#)
689 [10.5194/acp-6-3131-2006](http://dx.doi.org/10.5194/acp-6-3131-2006), 2006.
- 690 [Chang, C.-P., Millard, J. E., and Chen, G. T. J.: Gravitational Character of Cold](#)
691 [Surges during Winter MONEX, *Monthly Weather Review*, 111, 293-307,](#)
692 [10.1175/1520-0493\(1983\)111<0293:gcocsd>2.0.co;2](http://dx.doi.org/10.1175/1520-0493(1983)111<0293:gcocsd>2.0.co;2), 1983.
- 693 [Chang, C.-P., Harr, P. A., and Chen, H.-J.: Synoptic Disturbances over the](#)
694 [Equatorial South China Sea and Western Maritime Continent during Boreal Winter,](#)
695 [*Monthly Weather Review*, 133, 489-503, 10.1175/mwr-2868.1, 2005.](#)
- 696 [Crippa, P., Castruccio, S., Archer-Nicholls, S., Lebron, G. B., Kuwata, M., Thota, A.,](#)
697 [Sumin, S., Butt, E., Wiedinmyer, C., and Spracklen, D. V.: Population exposure to](#)
698 [hazardous air quality due to the 2015 fires in Equatorial Asia, *Scientific Reports*, 6,](#)
699 [37074, 10.1038/srep37074](http://dx.doi.org/10.1038/srep37074), 2016.
- 700 [Frankenberg, E., McKee, D., and Thomas, D.: Health consequences of forest fires](#)
701 [in Indonesia, *Demography*, 42, 109-129, 10.1353/dem.2005.0004, 2005.](#)
- 702 [Freitas, S. R., Longo, K. M., Chatfield, R., Latham, D., Silva Dias, M. A. F., Andreae,](#)
703 [M. O., Prins, E., Santos, J. C., Gielow, R., and Carvalho Jr, J. A.: Including the sub-grid](#)
704 [scale plume rise of vegetation fires in low resolution atmospheric transport models,](#)
705 [*Atmos. Chem. Phys.*, 7, 3385-3398, 10.5194/acp-7-3385-2007, 2007.](#)
- 706 [Fujii, Y., Iriana, W., Oda, M., Puriwigati, A., Tohno, S., Lestari, P., Mizohata, A., and](#)
707 [Huboyo, H. S.: Characteristics of carbonaceous aerosols emitted from peatland fire in](#)
708 [Riau, Sumatra, Indonesia, *Atmospheric Environment*, 87, 164-169,](#)
709 <http://dx.doi.org/10.1016/j.atmosenv.2014.01.037>, 2014.
- 710 [Ge, C., Wang, J., and Reid, J. S.: Mesoscale modeling of smoke transport over the](#)
711 [Southeast Asian Maritime Continent: coupling of smoke direct radiative effect below](#)
712 [and above the low-level clouds, *Atmos. Chem. Phys.*, 14, 159-174, 10.5194/acp-14-](#)
713 [159-2014](http://dx.doi.org/10.5194/acp-14-159-2014), 2014.
- 714 [Grandey, B. S., Lee, H. H., and Wang, C.: Radiative effects of interannually varying](#)
715 [vs. interannually invariant aerosol emissions from fires, *Atmos. Chem. Phys.*, 16,](#)
716 [14495-14513, 10.5194/acp-16-14495-2016](http://dx.doi.org/10.5194/acp-16-14495-2016), 2016.
- 717 [Grell, G. A., Peckham, S. E., Schmitz, R., McKeen, S. A., Frost, G., Skamarock, W. C.,](#)
718 [and Eder, B.: Fully coupled "online" chemistry within the WRF model, *Atmospheric*](#)
719 [Environment, 39, 6957-6975, 10.1016/j.atmosenv.2005.04.027, 2005.](#)
- 720 [Grell, G. A. and Freitas, S. R.: A scale and aerosol aware stochastic convective](#)
721 [parameterization for weather and air quality modeling, *Atmos. Chem. Phys.*, 14,](#)
722 [5233-5250, 10.5194/acp-14-5233-2014](http://dx.doi.org/10.5194/acp-14-5233-2014), 2014.
- 723 [Hodzic, A., and Duvel, J. P.: Impact of Biomass Burning Aerosols on the Diurnal](#)
724 [Cycle of Convective Clouds and Precipitation Over a Tropical Island, *Journal of*](#)

Deleted: Ackermann, I. J., Hass, H., Memmesheimer, M., Ebel, A., Binkowski, F. S., and Shankar, U.: Modal aerosol dynamics model for Europe: development and first applications, *Atmospheric Environment*, 32, 2981-2999, [http://dx.doi.org/10.1016/S1352-2310\(98\)00006-5](http://dx.doi.org/10.1016/S1352-2310(98)00006-5), 1998.¶

Andreae, M. O., and Gelencsér, A.: Black carbon or brown carbon? The nature of light-absorbing carbonaceous aerosols, *Atmos. Chem. Phys.*, 6, 3131-3148, 10.5194/acp-6-3131-2006, 2006.¶

Chang, C.-P., Millard, J. E., and Chen, G. T. J.: Gravitational Character of Cold Surges during Winter MONEX, *Monthly Weather Review*, 111, 293-307, 10.1175/1520-0493(1983)111<0293:gcocsd>2.0.co;2, 1983.¶

Chang, C.-P., Harr, P. A., and Chen, H.-J.: Synoptic Disturbances over the Equatorial South China Sea and Western Maritime Continent during Boreal Winter, *Monthly Weather Review*, 133, 489-503, 10.1175/mwr-2868.1, 2005.¶

Crippa, P., Castruccio, S., Archer-Nicholls, S., Lebron, G. B., Kuwata, M., Thota, A., Sumin, S., Butt, E., Wiedinmyer, C., and Spracklen, D. V.: Population exposure to hazardous air quality due to the 2015 fires in Equatorial Asia, *Scientific Reports*, 6, 37074, 10.1038/srep37074, 2016.¶

Frankenberg, E., McKee, D., and Thomas, D.: Health consequences of forest fires in Indonesia, *Demography*, 42, 109-129, 10.1353/dem.2005.0004, 2005.¶

Freitas, S. R., Longo, K. M., Chatfield, R., Latham, D., Silva Dias, M. A. F., Andreae, M. O., Prins, E., Santos, J. C., Gielow, R., and Carvalho Jr, J. A.: Including the sub-grid scale plume rise of vegetation fires in low resolution atmospheric transport models, *Atmos. Chem. Phys.*, 7, 3385-3398, 10.5194/acp-7-3385-2007, 2007.¶

Fujii, Y., Iriana, W., Oda, M., Puriwigati, A., Tohno, S., Lestari, P., Mizohata, A., and Huboyo, H. S.: Characteristics of carbonaceous aerosols emitted from peatland fire in Riau, Sumatra, Indonesia, *Atmospheric Environment*, 87, 164-169, <http://dx.doi.org/10.1016/j.atmosenv.2014.01.037>, 2014.¶

Ge, C., Wang, J., and Reid, J. S.: Mesoscale modeling of smoke transport over the Southeast Asian Maritime Continent: coupling of smoke direct radiative effect below and above the low-level clouds, *Atmos. Chem. Phys.*, 14, 159-174, 10.5194/acp-14-159-2014, 2014.¶

Grandey, B. S., Lee, H. H., and Wang, C.: Radiative effects of interannually varying vs. interannually invariant aerosol emissions from fires, *Atmos. Chem. Phys.*, 16, 14495-14513, 10.5194/acp-16-14495-2016, 2016.¶

Grell, G. A., Peckham, S. E., Schmitz, R., McKeen, S. A., Frost, G., Skamarock, W. C., and Eder, B.: Fully coupled "online" chemistry within the WRF model, *Atmospheric Environment*, 39, 6957-6975, 10.1016/j.atmosenv.2005.04.027, 2005.¶

Grell, G. A., and Freitas, S. R.: A scale and aerosol aware stochastic convective parameterization for weather and air quality modeling, *Atmos. Chem. Phys.*, 14, 5233-5250, 10.5194/acp-14-5233-2014, 2014.¶

... [1]

§60 [Geophysical Research: Atmospheres](#), 123, 1017-1036, 10.1002/2017JD027521,
 §61 [2017](#).
 §62 [Huffman, G. J., Bolvin, D. T., Nelkin, E. I., Wolff, D. B., Adler, R. F., Gu, G., Hong, Y.,](#)
 §63 [Bowman, K. P., and Stocker, E. F.: The TRMM Multisatellite Precipitation Analysis](#)
 §64 [\(TMPA\): Quasi-Global, Multiyear, Combined-Sensor Precipitation Estimates at Fine](#)
 §65 [Scales. *Journal of Hydrometeorology*, 8, 38-55, 10.1175/JHM560.1, 2007.](#)
 §66 [Iacono, M. J., Delamere, J. S., Mlawer, E. J., Shephard, M. W., Clough, S. A., and](#)
 §67 [Collins, W. D.: Radiative forcing by long-lived greenhouse gases: Calculations with](#)
 §68 [the AER radiative transfer models. *Journal of Geophysical Research: Atmospheres*,](#)
 §69 [113, 10.1029/2008JD009944, 2008.](#)
 §70 [Ichikawa, H., and Yasunari, T.: Time-Space Characteristics of Diurnal Rainfall](#)
 §71 [over Borneo and Surrounding Oceans as Observed by TRMM-PR. *Journal of Climate*,](#)
 §72 [19, 1238-1260, 10.1175/jcli3714.1, 2006.](#)
 §73 [Jeong, G. R., and Wang, C.: Climate effects of seasonally varying Biomass Burning](#)
 §74 [emitted Carbonaceous Aerosols \(BBCA\). *Atmos. Chem. Phys.*, 10, 8373-8389,](#)
 §75 [10.5194/acp-10-8373-2010, 2010.](#)
 §76 [Jiang, J. H., Su, H., Huang, L., Wang, Y., Massie, S., Zhao, B., Omar, A., and Wang, Z.:](#)
 §77 [Contrasting effects on deep convective clouds by different types of aerosols. *Nature*](#)
 §78 [Communications, 9, 3874, 10.1038/s41467-018-06280-4, 2018.](#)
 §79 [Koh, T.-Y., and Teo, C.-K.: TOWARD A MESOSCALE OBSERVATION NETWORK IN](#)
 §80 [SOUTHEAST ASIA. *Bulletin of the American Meteorological Society*, 90, 481-488,](#)
 §81 [10.1175/2008bams2561.1, 2009.](#)
 §82 [Kunii, O., Kanagawa, S., Yajima, I., Hisamatsu, Y., Yamamura, S., Amagai, T., and](#)
 §83 [Ismail, I. T. S.: The 1997 Haze Disaster in Indonesia: Its Air Quality and Health](#)
 §84 [Effects. *Archives of Environmental Health: An International Journal*, 57, 16-22,](#)
 §85 [10.1080/00039890209602912, 2002.](#)
 §86 [Kurokawa, I., Ohara, T., Morikawa, T., Hanayama, S., Janssens-Maenhout, G.,](#)
 §87 [Fukui, T., Kawashima, K., and Akimoto, H.: Emissions of air pollutants and](#)
 §88 [greenhouse gases over Asian regions during 2000-2008: Regional Emission](#)
 §89 [inventory in ASia \(REAS\) version 2. *Atmos. Chem. Phys.*, 13, 11019-11058,](#)
 §90 [10.5194/acp-13-11019-2013, 2013.](#)
 §91 [Lee, H.-H., Bar-Or, R. Z., and Wang, C.: Biomass burning aerosols and the low-](#)
 §92 [visibility events in Southeast Asia. *Atmos. Chem. Phys.*, 17, 965-980, 10.5194/acp-](#)
 §93 [17-965-2017, 2017.](#)
 §94 [Lee, H.-H., Iraqi, O., Gu, Y., Yim, S. H. L., Chulakadabba, A., Tonks, A. Y. M., Yang,](#)
 §95 [Z., and Wang, C.: Impacts of air pollutants from fire and non-fire emissions on the](#)
 §96 [regional air quality in Southeast Asia. *Atmos. Chem. Phys.*, 18, 6141-6156,](#)
 §97 [10.5194/acp-18-6141-2018, 2018.](#)
 §98 [Lee, H.-H., Iraqi, O., and Wang, C.: The Impact of Future Fuel Consumption on](#)
 §99 [Regional Air Quality in Southeast Asia. *Scientific Reports*, 9, 2648, 10.1038/s41598-](#)
 §00 [019-39131-3, 2019.](#)
 §01 [Lin, J. C., Matsui, T., Pielke Sr., R. A., and Kummerow, C.: Effects of biomass-](#)
 §02 [burning-derived aerosols on precipitation and clouds in the Amazon Basin: a](#)
 §03 [satellite-based empirical study. *Journal of Geophysical Research: Atmospheres*, 111,](#)
 §04 [10.1029/2005jd006884, 2006.](#)

905 [Lin, N.-H., Tsay, S.-C., Maring, H. B., Yen, M.-C., Sheu, G.-R., Wang, S.-H., Chi, K. H.,](#)
906 [Chuang, M.-T., Ou-Yang, C.-F., Fu, J. S., Reid, J. S., Lee, C.-T., Wang, L.-C., Wang, J.-L.,](#)
907 [Hsu, C. N., Sayer, A. M., Holben, B. N., Chu, Y.-C., Nguyen, X. A., Sopajaree, K., Chen, S.-](#)
908 [J., Cheng, M.-T., Tsuang, B.-J., Tsai, C.-J., Peng, C.-M., Schnell, R. C., Conway, T., Chang,](#)
909 [C.-T., Lin, K.-S., Tsai, Y. I., Lee, W.-J., Chang, S.-C., Liu, J.-J., Chiang, W.-L., Huang, S.-J.,](#)
910 [Lin, T.-H., and Liu, G.-R.: An overview of regional experiments on biomass burning](#)
911 [aerosols and related pollutants in Southeast Asia: From BASE-ASIA and the Dongsha](#)
912 [Experiment to 7-SEAS, Atmospheric Environment, 78, 1-19,](#)
913 <http://dx.doi.org/10.1016/j.atmosenv.2013.04.066>, 2013.

914 [Lo, J. C. F., and Orton, T.: The general features of tropical Sumatra Squalls,](#)
915 [Weather, 71, 175-178, 10.1002/wea.2748](#), 2016.

916 [Miettinen, J., Shi, C., and Liew, S. C.: Deforestation rates in insular Southeast Asia](#)
917 [between 2000 and 2010, Global Change Biology, 17, 2261-2270, 10.1111/j.1365-](#)
918 [2486.2011.02398.x](#), 2011.

919 [Mlawer, E. J., Taubman, S. J., Brown, P. D., Iacono, M. J., and Clough, S. A.:](#)
920 [Radiative transfer for inhomogeneous atmospheres: RRTM, a validated correlated-k](#)
921 [model for the longwave, Journal of Geophysical Research: Atmospheres, 102, 16663-](#)
922 [16682, 10.1029/97JD00237](#), 1997.

923 [Morrison, H., Curry, J. A., and Khvorostyanov, V. I.: A New Double-Moment](#)
924 [Microphysics Parameterization for Application in Cloud and Climate Models. Part I:](#)
925 [Description, Journal of the Atmospheric Sciences, 62, 1665-1677,](#)
926 [10.1175/jas3446.1](#), 2005.

927 [Morrison, H., Thompson, G., and Tatarskii, V.: Impact of Cloud Microphysics on](#)
928 [the Development of Trailing Stratiform Precipitation in a Simulated Squall Line:](#)
929 [Comparison of One- and Two-Moment Schemes, Monthly Weather Review, 137,](#)
930 [991-1007, 10.1175/2008mwr2556.1](#), 2009.

931 [Nakanishi, M., and Niino, H.: Development of an Improved Turbulence Closure](#)
932 [Model for the Atmospheric Boundary Layer, Journal of the Meteorological Society of](#)
933 [Japan, Ser. II, 87, 895-912, 10.2151/jmsj.87.895](#), 2009.

934 [National Centers for Environmental Prediction, N. W. S. N. U. S. D. o. C.: NCEP](#)
935 [FNL Operational Model Global Tropospheric Analyses, continuing from July 1999,](#)
936 [10.5065/D6M043C6](#), 2000.

937 [Oki, T., and Musiake, K.: Seasonal Change of the Diurnal Cycle of Precipitation](#)
938 [over Japan and Malaysia, Journal of Applied Meteorology, 33, 1445-1463,](#)
939 [10.1175/1520-0450\(1994\)033<1445:scotdc>2.0.co;2](#), 1994.

940 [Ramanathan, V., Crutzen, P. J., Lelieveld, J., Mitra, A. P., Althausen, D., Anderson,](#)
941 [J., Andreae, M. O., Cantrell, W., Cass, G. R., Chung, C. E., Clarke, A. D., Coakley, J. A.,](#)
942 [Collins, W. D., Conant, W. C., Dulac, F., Heintzenberg, J., Heymsfield, A. J., Holben, B.,](#)
943 [Howell, S., Hudson, J., Jayaraman, A., Kiehl, J. T., Krishnamurti, T. N., Lubin, D.,](#)
944 [McFarquhar, G., Novakov, T., Ogren, J. A., Podgorny, I. A., Prather, K., Priestley, K.,](#)
945 [Prospero, J. M., Quinn, P. K., Rajeev, K., Rasch, P., Rupert, S., Sadourny, R., Satheesh, S.](#)
946 [K., Shaw, G. E., Sheridan, P., and Valero, F. P. J.: Indian Ocean Experiment: An](#)
947 [integrated analysis of the climate forcing and effects of the great Indo-Asian haze,](#)
948 [Journal of Geophysical Research: Atmospheres, 106, 28371-28398,](#)
949 [10.1029/2001jd900133](#), 2001.

950 [Ramanathan, V., and Carmichael, G.: Global and regional climate changes due to](#)
951 [black carbon, *Nature Geosci.*, 1, 221-227, 2008.](#)
952 [Rosenfeld, D.: TRMM observed first direct evidence of smoke from forest fires](#)
953 [inhibiting rainfall, *Geophysical Research Letters*, 26, 3105-3108,](#)
954 [10.1029/1999gl006066, 1999.](#)
955 [Satheesh, S. K., and Ramanathan, V.: Large differences in tropical aerosol forcing](#)
956 [at the top of the atmosphere and Earth's surface, *Nature*, 405, 60-63,](#)
957 [10.1038/35011039, 2000.](#)
958 [Schell, B., Ackermann, I. J., Hass, H., Binkowski, F. S., and Ebel, A.: Modeling the](#)
959 [formation of secondary organic aerosol within a comprehensive air quality model](#)
960 [system, *Journal of Geophysical Research: Atmospheres* \(1984–2012\), 106, 28275-](#)
961 [28293, 2001.](#)
962 [Sekiguchi, M., Nakajima, T., Suzuki, K., Kawamoto, K., Higurashi, A., Rosenfeld, D.,](#)
963 [Sano, I., and Mukai, S.: A study of the direct and indirect effects of aerosols using](#)
964 [global satellite data sets of aerosol and cloud parameters, *Journal of Geophysical*](#)
965 [Research: Atmospheres](#), 108, 4699, 10.1029/2002JD003359, 2003.
966 [Shi, H., Jiang, Z., Zhao, B., Li, Z., Chen, Y., Gu, Y., Jiang, J. H., Lee, M., Liou, K.-N.,](#)
967 [Neu, J. L., Payne, V. H., Su, H., Wang, Y., Witek, M., and Worden, J.: Modeling Study of](#)
968 [the Air Quality Impact of Record-Breaking Southern California Wildfires in](#)
969 [December 2017, *Journal of Geophysical Research: Atmospheres*, 124, 6554-6570,](#)
970 [10.1029/2019jd030472, 2019.](#)
971 [Stockwell, W. R., Kirchner, F., Kuhn, M., and Seefeld, S.: A new mechanism for](#)
972 [regional atmospheric chemistry modeling, *Journal of Geophysical Research:*](#)
973 [Atmospheres](#), 102, 25847-25879, 10.1029/97JD00849, 1997.
974 [Taylor, D.: Biomass burning, humans and climate change in Southeast Asia,](#)
975 [Biodivers Conserv](#), 19, 1025-1042, 10.1007/s10531-009-9756-6, 2010.
976 [Tewari, M., F. Chen, W. Wang, J. Dudhia, M. A. LeMone, K. Mitchell, M. Ek, G.](#)
977 [Gayno, J. Wegiel, and Cuenca, R. H.: Implementation and verification of the unified](#)
978 [NOAH land surface model in the WRF model, 20th conference on weather analysis](#)
979 [and forecasting/16th conference on numerical weather prediction, Seattle, WA,](#)
980 [U.S.A., 2004.](#)
981 [Tosca, M. G., Randerson, J. T., and Zender, C. S.: Global impact of smoke aerosols](#)
982 [from landscape fires on climate and the Hadley circulation, *Atmos. Chem. Phys.*, 13,](#)
983 [5227-5241, 10.5194/acp-13-5227-2013, 2013.](#)
984 [Wagner, A., Heinzeller, D., Wagner, S., Rummeler, T., and Kunstmann, H.: Explicit](#)
985 [Convection and Scale-Aware Cumulus Parameterizations: High-Resolution](#)
986 [Simulations over Areas of Different Topography in Germany, *Monthly Weather*](#)
987 [Review](#), 146, 1925-1944, 10.1175/mwr-d-17-0238.1, 2018.
988 [Wang, C.: A modeling study on the climate impacts of black carbon aerosols,](#)
989 [Journal of Geophysical Research: Atmospheres](#), 109, n/a-n/a,
990 [10.1029/2003JD004084, 2004.](#)
991 [Wang, C.: A modeling study of the response of tropical deep convection to the](#)
992 [increase of cloud condensation nuclei concentration: 1. Dynamics and microphysics,](#)
993 [Journal of Geophysical Research: Atmospheres](#), 110, D21211,
994 [10.1029/2004JD005720, 2005.](#)

995 [Wiedinmyer, C., Akagi, S. K., Yokelson, R. J., Emmons, L. K., Al-Saadi, J. A.,](#)
996 [Orlando, J. J., and Soja, A. J.: The Fire INventory from NCAR \(FINN\): a high resolution](#)
997 [global model to estimate the emissions from open burning, *Geosci. Model Dev.*, **4**,](#)
998 [625-641, 10.5194/gmd-4-625-2011, 2011.](#)
999 [Wu, P., Hara, M., Hamada, I.-i., Yamanaka, M. D., and Kimura, F.: Why a Large](#)
1000 [Amount of Rain Falls over the Sea in the Vicinity of Western Sumatra Island during](#)
1001 [Nighttime, *Journal of Applied Meteorology and Climatology*, **48**, 1345-1361,](#)
1002 [10.1175/2009jamc2052.1, 2009.](#)
1003 [Wu, R., Wen, Z., and He, Z.: ENSO Contribution to Aerosol Variations over the](#)
1004 [Maritime Continent and the Western North Pacific during 2000–10, *Journal of*](#)
1005 [Climate](#), **26**, 6541-6560, 10.1175/JCLI-D-12-00253.1, 2013.
1006 [Yi, L., and Lim, H.: Semi-Idealized COAMPS@* Simulations of Sumatra Squall](#)
1007 [Lines: the Role of Boundary Forcing, in: *Advances in Geosciences*, 111-124, 2006.](#)
1008 [Zhang, Y., Fan, J., Logan, T., Li, Z., and Homeyer, C. R.: Wildfire impact on](#)
1009 [environmental thermodynamics and severe convective storms, *Geophysical*](#)
1010 [Research Letters](#), **0**, 10.1029/2019gl084534, 2019.
1011 [Zhao, B., Gu, Y., Liou, K.-N., Wang, Y., Liu, X., Huang, L., Jiang, J. H., and Su, H.:](#)
1012 [Type-Dependent Responses of Ice Cloud Properties to Aerosols From Satellite](#)
1013 [Retrievals, *Geophysical Research Letters*, **45**, 3297-3306, 10.1002/2018gl077261,](#)
1014 [2018.](#)
1015
1016

Formatted: Indent: First line: 0.31"

1017
1018

Table 1. The case period of the selected cases in the Sumatra region (r1) and the Borneo region (r2)

Case name	Case period
r1c1	2008/08/10 0900 UTC ~ 2008/08/11 0300 UTC
r1c2	2008/08/19 0600 UTC ~ 2008/08/20 0000 UTC
r1c3	2008/09/23 0900 UTC ~ 2008/09/24 0000 UTC
r2c1	2008/08/05 0900 UTC ~ 2008/08/06 0300 UTC
r2c2	2008/09/17 0600 UTC ~ 2008/09/17 2100 UTC
r2c3	2008/09/22 0300 UTC ~ 2008/09/23 0000 UTC

1019
1020
1021

1022

Table 2. The fire periods in the two study regions

The Sumatra region (r1)	The Borneo region (r2)
6/10/2008 ~ 6/20/2008	6/21/2008 ~ 6/27/2008
6/25/2008 ~ 6/28/2008	8/1/2008 ~ 8/8/2008
7/4/2008 ~ 7/7/2008	9/10/2008 ~ 9/30/2008
7/27/2008 ~ 8/20/2008	
9/17/2008 ~ 9/27/2008	

1023

1024

1025 Table 3. The mean differences in percentage of FFBB to FF (i.e. $(FFBB-FF)/FF \times 100\%$)
 1026 for each selected case over the main convection area in the Sumatra region (r1) and the
 1027 Borneo region (r2). Qc, Qi, Qr, Qs and Qg represents cloud, ice, rain, snow, and graupel
 1028 mass concentration respectively. Qnc, Qni, Qnr, Qns and Qng means number
 1029 concentration for each hydrometeor.

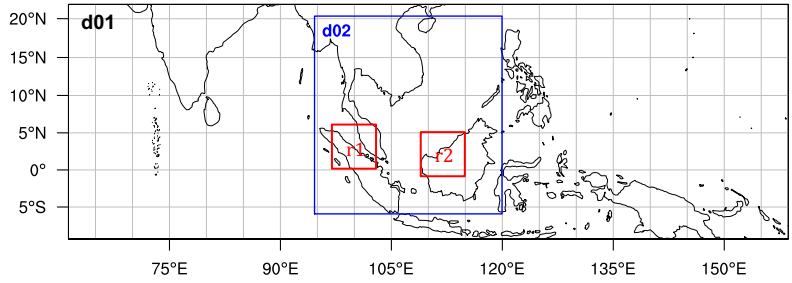
Case	Qc	Qi	Qr	Qs	Qg	Qnc	Qni	Qnr	Qns	Qng
r1c1	8%	27%	49%	62%	48%	248%	55%	-41%	33%	39%
r1c2	20%	-6%	-15%	-25%	1%	349%	-1%	-45%	-11%	-6%
r1c3	18%	10%	-10%	3%	5%	311%	4%	-50%	11%	-6%
r2c1	27%	1%	-6%	-5%	-4%	703%	3%	-59%	4%	-5%
r2c2	22%	10%	64%	69%	58%	337%	24%	-32%	17%	57%
r3c3	8%	10%	19%	60%	-2%	409%	-5%	-66%	8%	-12%

1030

1031 Table 4. The averaged precipitation (mm 3hrs⁻¹) of FFBB and FF for each selected case
 1032 over the main convection area in the Sumatra region (r1) and the Borneo region (r2).
 1033 Parentheses in the third column show the difference in percentage of FFBB to FF (i.e.
 1034 (FFBB-FF)/FF × 100%).
 1035

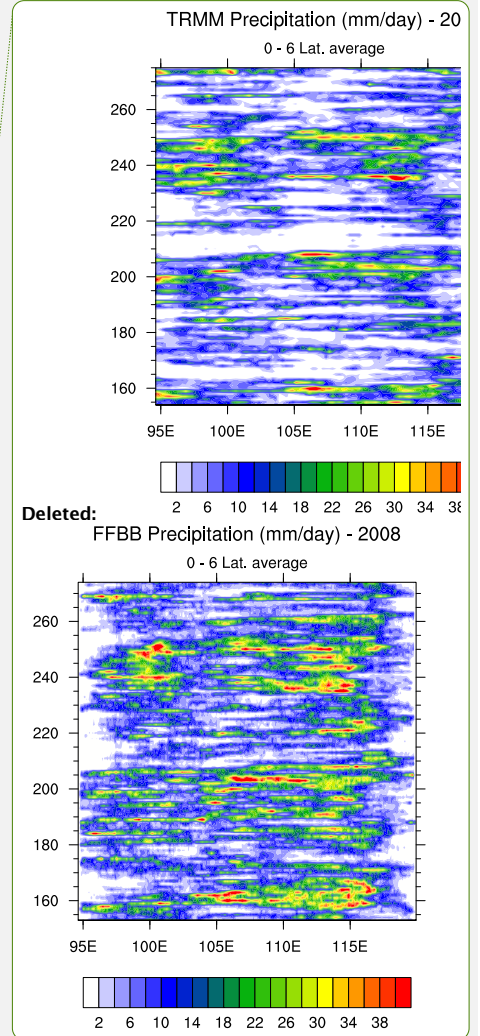
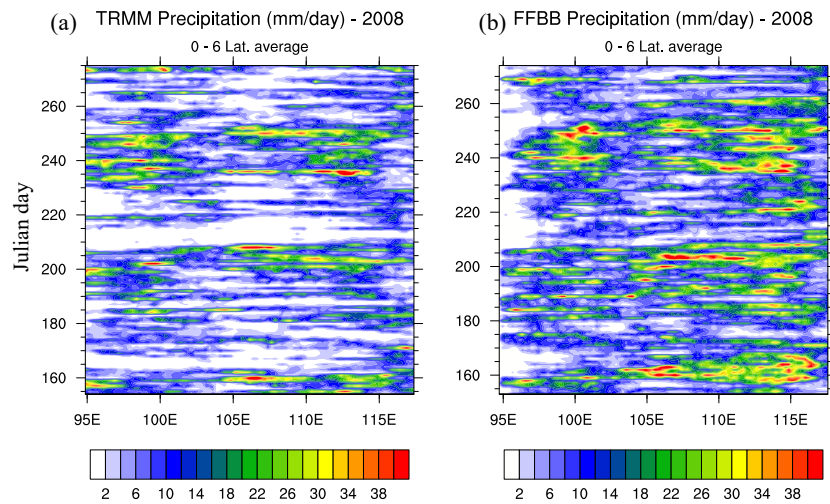
Case	FF	FFBB
r1c1	1.33±0.47	2.74±1.21 (+106%)
r1c2	2.97±1.42	3.05±1.49 (+3%)
r1c3	4.32±1.84	3.98±2.18 (-8%)
r2c1	3.73±2.64	3.07±1.21 (-18%)
r2c2	1.88±0.53	3.97±1.47 (+111%)
r3c3	0.54±0.53	1.10±1.02 (+103%)

1036
 1037



1038
1039
1040
1041
1042
1043
1044

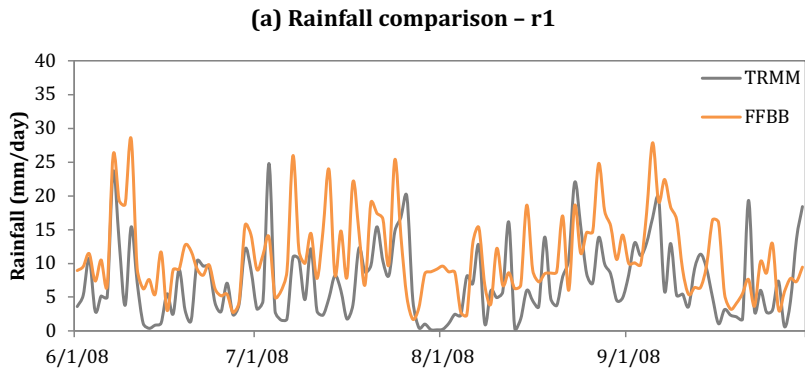
Figure 1. Domain configuration for WRF-Chem simulations. Domain 1 (d01) has a resolution of 25 km, while Domain 2 (d02) has a resolution of 5 km. Two red boxes indicate the two study regions: the Sumatra region (r1) and the Borneo region (r2).



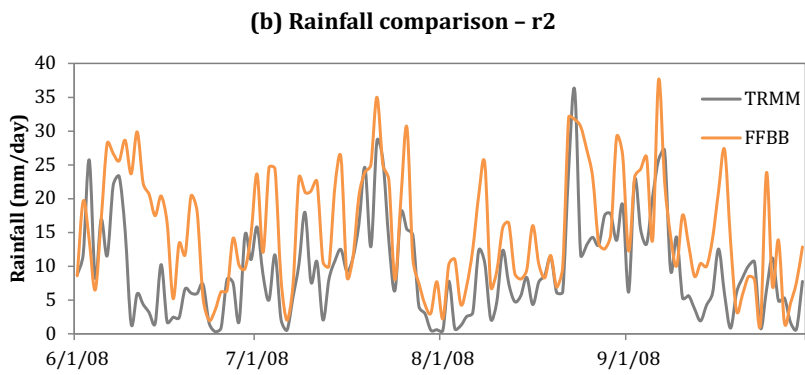
1045
1046
1047
1048
1049

Figure 2. Hovmöller (time versus longitude) plot of daily precipitation (mm day^{-1}) from 1 June 2008 to 30 September 2008 from:(a) Tropical Rainfall Measuring Mission (TRMM) and (b) FFBB. Latitude average is from 0° to 6°N .

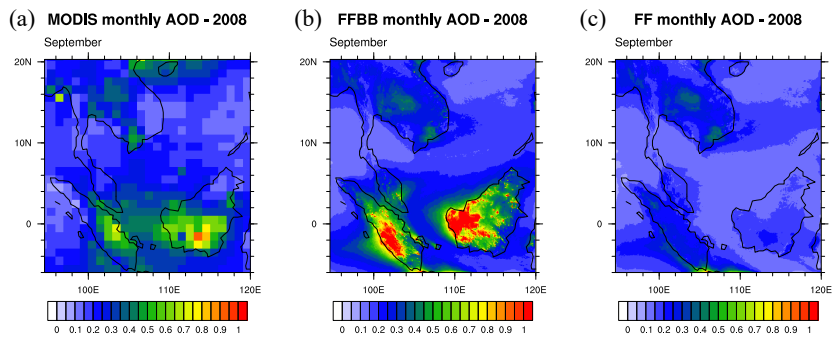
1052



1053

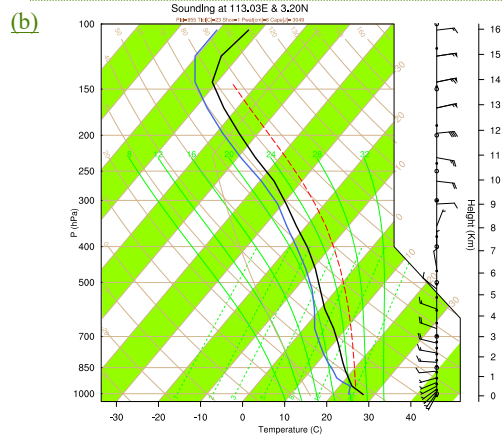
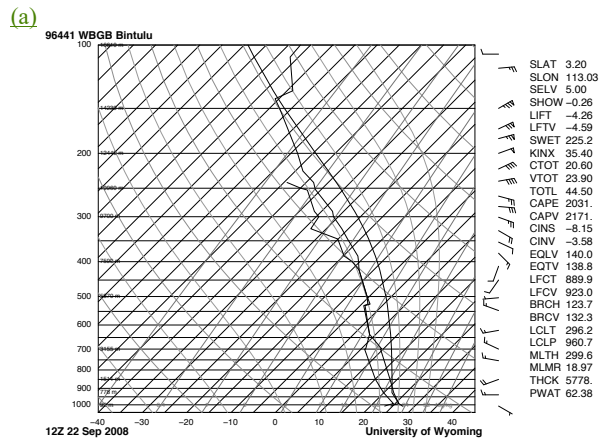


1054 Figure 3. Time series of area-averaged daily rainfall (mm day^{-1}) from Tropical Rainfall
1055 Measuring Mission (TRMM) and FFBB over (a) the Sumatra region (r1) and (b) the
1056 Borneo region (r2).
1057



1058
 1059 Figure 4. Monthly aerosol optical depth (AOD) in September 2008 from (a) Moderate
 1060 Resolution Imaging Spectroradiometer (MODIS), (b) FFBB, and (c) FF.
 1061
 1062

1063



1064

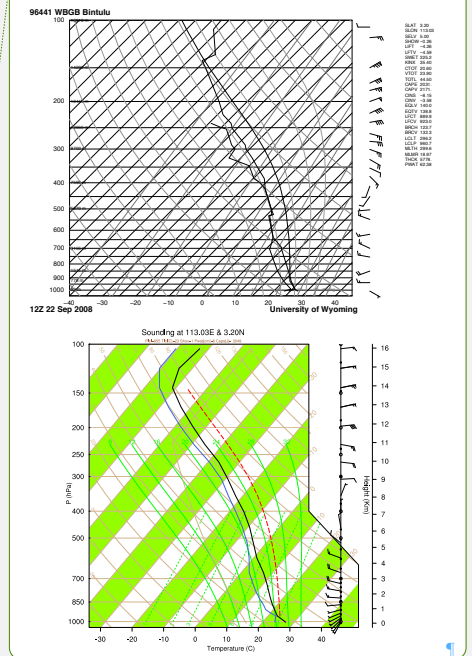
1065

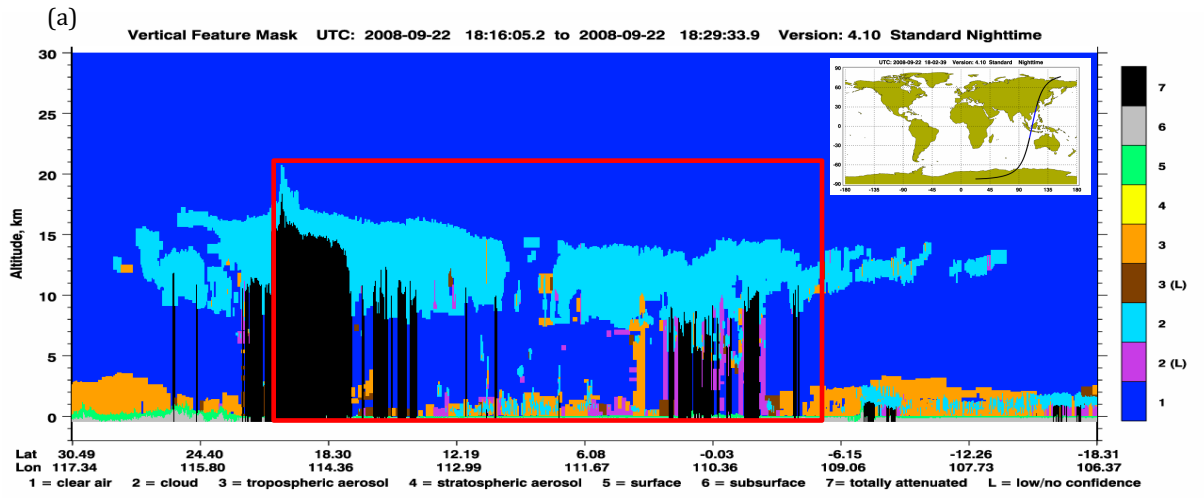
1066

1067

Figure 5. (a) Sounding profile observed at Bintulu Airport, Malaysia (113.03° E, 3.20° N) at 12 UTC on 22 September 2008. (b) Modeled sounding profile in FFBB at the same location and time as (a).

Deleted: <object><object>

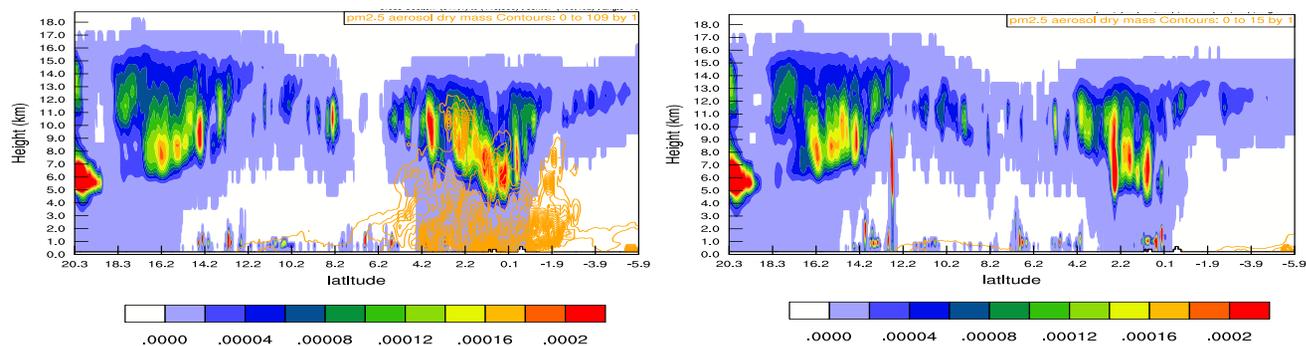




(b)

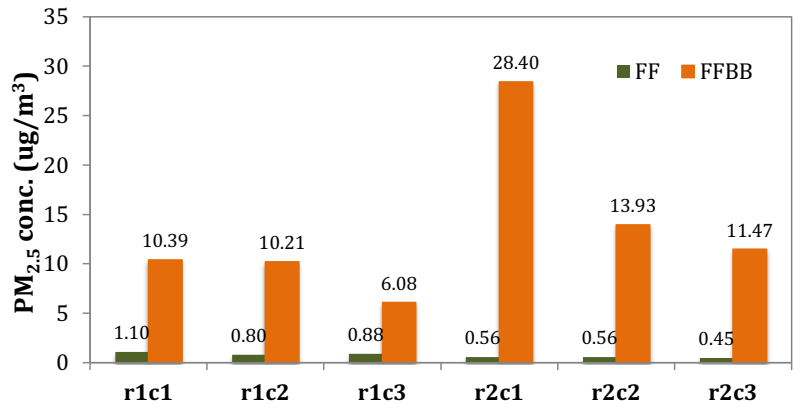
(c)

1071
 1072
 1073



1074
 1075
 1076
 1077
 1078

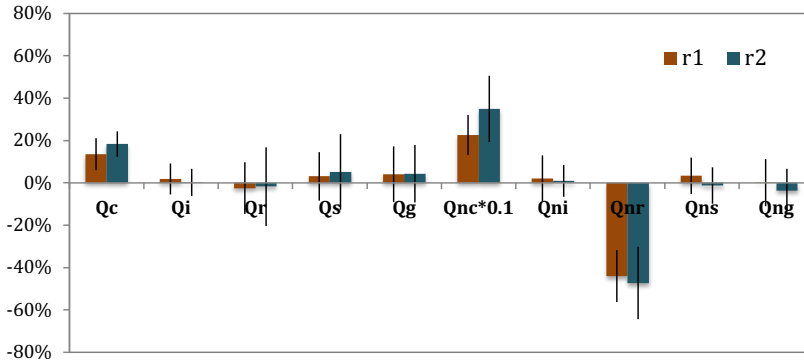
Figure 6 (a) The vertical structure of cloud retrieved from the Cloud-Aerosol Lidar and Infrared Pathfinder Satellite Observation (CALIPSO) on September 22, 2008. (b)-(c) The sum of simulated hydrometeor mixing ratio (shaded; kg kg^{-1}) and $\text{PM}_{2.5}$ concentration (contour; $\mu\text{g m}^{-3}$) in FFBB and FF, respectively. The profile domain of (b) and (c) is corresponding to the red rectangle in (a).



1079
 1080
 1081
 1082

Figure 7. The mean PM_{2.5} concentration (µg m⁻³) in FF and FFBB for selected cases in the Sumatra region (r1) and the Borneo region (r2).

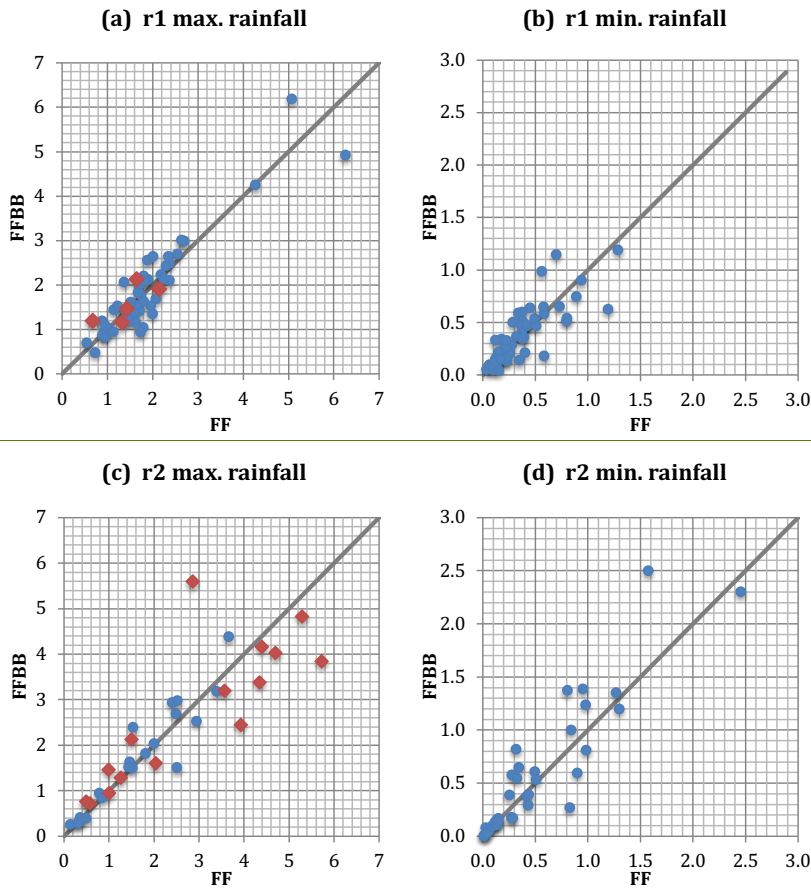
1083
1084



1085
1086
1087
1088
1089
1090
1091
1092

Figure 8. The mean differences in percentage of FFBB to FF (i.e. $(FFBB-FF)/FF \times 100\%$) over all convective cases during the fire periods in the Sumatra region (r1) and the Borneo region (r2). Qc, Qi, Qr, Qs and Qg represents cloud, ice, rain, snow, and graupel mass concentration, respectively. Qnc, Qni, Qnr, Qns and Qng means number concentration for each hydrometeor. The error bars represent one standard deviation.

1093



1094

1095

1096

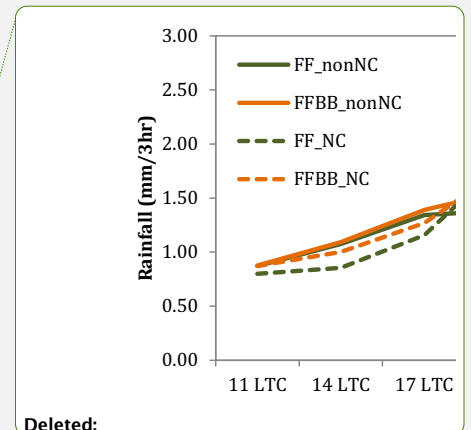
1097

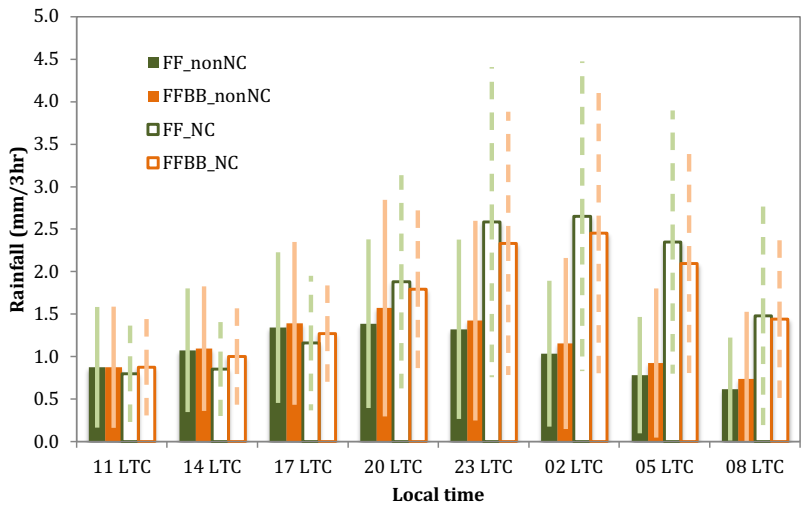
1098

1099

1100

Figure 9. The scatterplots of daily maximum and minimum convective rainfall ($\text{mm } 3\text{hr}^{-1}$) during the fire periods in in the Sumatra region (r1) and the Borneo region (r2). Red diamonds in (a) and (c) indicate that the maximum convective rainfall conducts in the midnight or early morning.



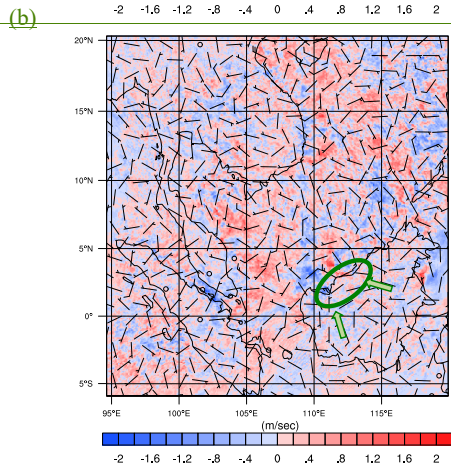
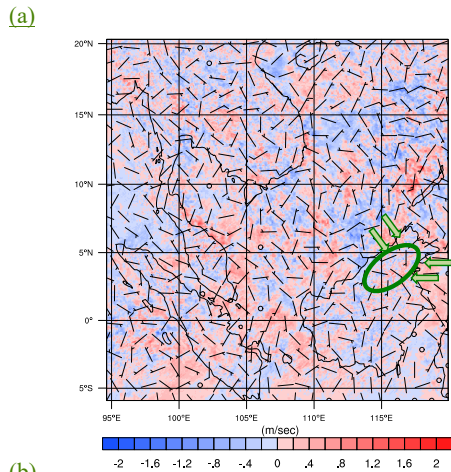


Deleted: precipitation

1102
 1103
 1104
 1105
 1106
 1107

Figure 10. The diurnal time series of rainfall averaged over the Borneo region (r2) for nocturnal convections (NC) and non- nocturnal convections (non-NC) during fire periods in FF and FFBB. The error bars denote the standard deviation of the rainfall.

1109

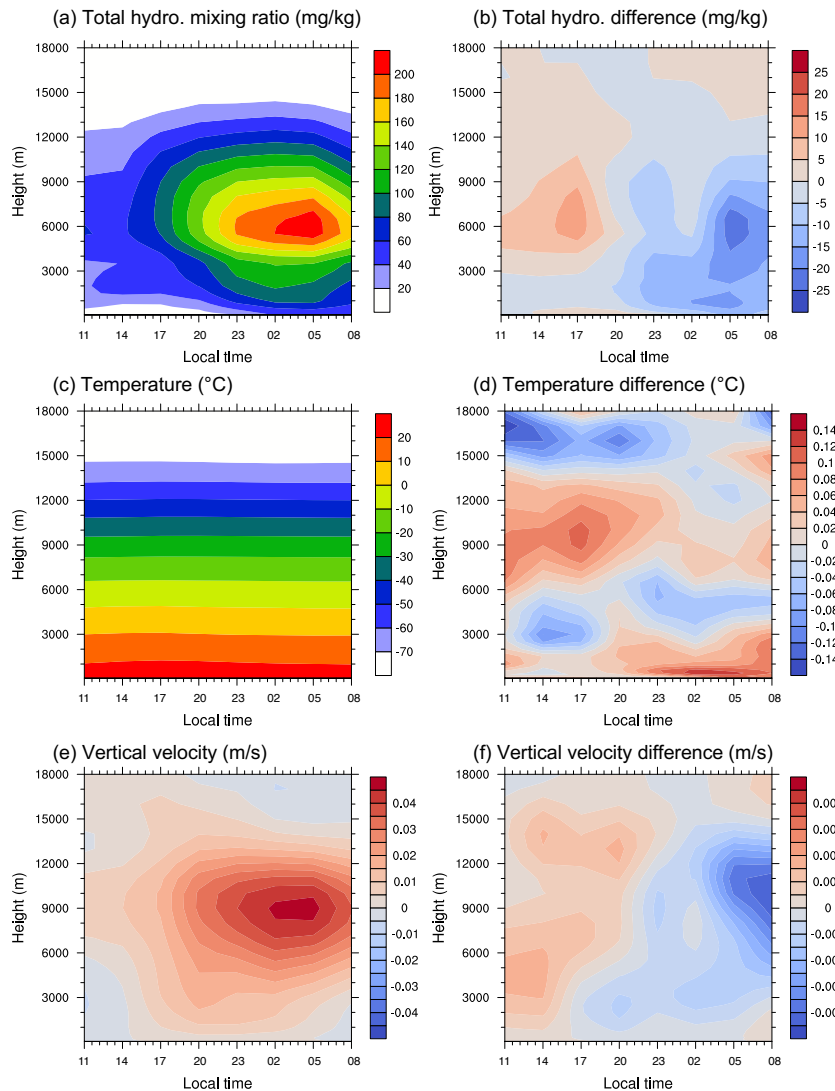


1110

1111 Figure 11. The mean wind field differences of FFBB and FF (FFBB-FF) at (a) 20 LTC for
1112 non-nocturnal cases and (b) 02 LTC for nocturnal cases in the Borneo region (r2). The green
1113 circle indicates the location of convections occurred. The green arrows mean the mean flow
1114 of sea breeze in (a) and land breeze in (b). The magnitude of wind barbs is 10 times higher
1115 than the real value.

1116

1117



1118
1119

1120
1121

1122

1123

1124

1125

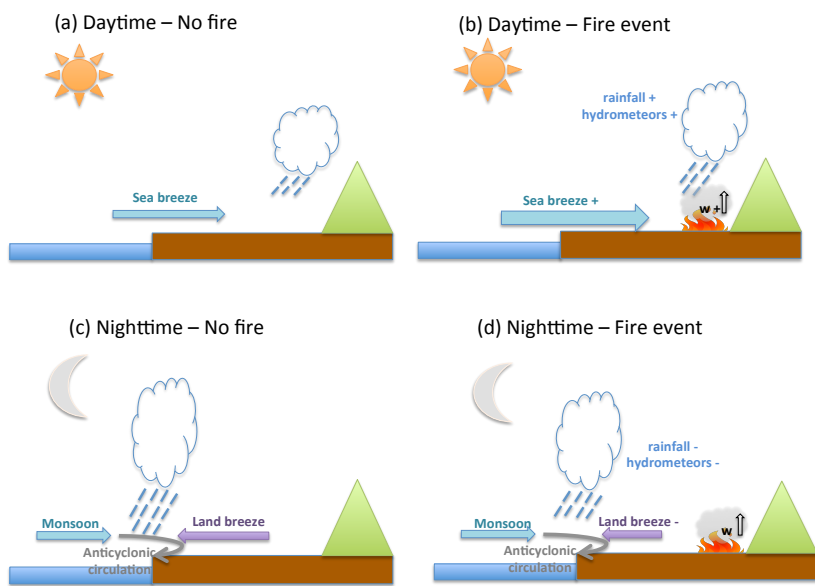
1126

1127

Figure 12. Diurnal evolution of vertical profiles over the Borneo region (r_2) in FF for (a) total hydrometeor mixing ratio (mg kg^{-1}), (c) temperature ($^{\circ}\text{C}$), and (e) vertical velocity (m s^{-1}). Data are averaged all the nocturnal convections. (b), (d), and (f) is the differences between FF and FFBB (FFBB-FF) for each parameter.

Deleted: 11

1129



1130

1131 Figure 13. Schematics of diurnal rainfall/convection activity over the western Borneo. (a)
1132 and (b) illustrate the formation of convection during the daytime without and with fire event,
1133 respectively. (c) and (d) are the same as (a) and (b) but in the nighttime.

1134

Deleted: 12